

Marian Klasztorny<sup>a\*</sup>, Daniel B. Nycz<sup>1</sup>

<sup>1</sup> Institute of Technology, Jan Grodek State University in Sanok, ul. A. Mickiewicza 21, 38-500 Sanok, Poland

<sup>a</sup> At present: professor emeritus in civil and mechanical engineering

\*Corresponding author. E-mail: m.klasztorny@gmail.com

Received (Otrzymano) 28.01.2023

## NOVEL RHEOLOGICAL MODELLING OF THERMOSETS AND UNIDIRECTIONAL MONOTROPIC FIBRE-REINFORCED THERMOSET MATRIX COMPOSITES

A refined, fully analytical rheological modelling of thermosetting polymers and unidirectional monotropic fibre-reinforced thermoset matrix (UFRT) composites is presented. New polymers and composites under normal conditions, fully relaxed from curing and post-curing stresses, are modelled. The theory includes quasi-static short-term/medium-term/long-term reversible rheological processes. Thermosets are isotropic materials exhibiting linearly viscoelastic shear strains and linearly elastic bulk strains. Fibres are monotropic (transversely isotropic) and linearly elastic materials. A generic function well reproducing the viscoelastic characteristics of thermosets and UFRT composites is a Mittag-Leffler fractional exponential function in an integral form. Coupled/uncoupled standard/inverse constitutive equations of linear rheology are formulated for thermosets and UFRT composites. The equations are mutually analytically transformable. New rheological models (coded H-R/H) for thermosets and UFRT composites are described by the smallest possible number of material constants. The thermoset is described by two independent elastic constants and three independent viscoelastic constants. The homogenized UFRT composite is described by five independent elastic constants and four independent viscoelastic constants, whereby two viscoelastic constants are common to the matrix and the composite. An improved homogenization theory of UFRT composites, based on analytical solutions of the selected tasks of the theory of linear elasticity, is formulated for monotropic fibres and positively validated experimentally. The viscoelastic constants of the thermoset are calculated analytically in an iterative loop using a long-term unidirectional tension creep experimental test. The viscoelastic constants of the UFRT composite are calculated analytically employing H-R/H shear/quasi-shear storage compliances and VECP (the viscoelastic-elastic correspondence principle) shear/quasi-shear storage compliances. The H-R/H rheological model was validated numerically for selected UFRT composites. The validation tests were performed on the enhanced reliability UFRT composites reported by Soden, Hinton, and Kaddour (Composites Science and Technology, 1998, 2002).

**Keywords:** thermoset, monotropic fibre-reinforced thermoset matrix composite, elasticity, rheology, homogenization, fractional exponential generic function, material modelling, identification, simulation, validation

### INTRODUCTION

Laminates with thermosetting matrices reinforced with glass or carbon fibres are commonly used in automotive, aerospace/space, civil or marine/naval structures. In the design of these structures, relatively low stress levels leading to linearly elastic reversible processes are allowed. The effects of the viscoelastic characteristics of polymer matrices, temperature and aging are taken into account by partial safety factors. Development of the rheological modelling of thermosetting resins and fibre-reinforced polymer matrix composites is therefore expected by engineers.

Each lamina in structural laminates is a unidirectional long fibre-reinforced thermoset matrix (UFRT) composite. A thermosetting resin matrix, mostly the epoxy- or polyester type, after the curing and post-curing processes have been completed, is a solid material exhibiting substantial viscoelastic or viscoelastic-plastic deformations depending on the stress level, temperature level and time, e.g. Ref. [1]. The viscoelas-

tic strains of thermosetting matrices can induce significant stress redistributions or undesirable deformations of laminates over a short/medium/long lifetime.

A study of the literature on the elastic-viscoelastic or elastic-viscoelastic-plastic response of new thermosets and UFRT composites, fully relaxed after manufacturing processes, subjected to long-term mechanical/thermal loads was presented in [2]. Therefore, in this study the literature review is presented in an abridged version but supplemented with more publications.

The rheological models of thermosets can be reflected by mechanical systems composed of Hooke (H), Kelvin (K), Maxwell (M), Newton (N), Rabinovitch (R), Schapery (S) and other elements, in serial, parallel or serial/parallel connections. The H, K, M, and N elements are defined classically. Element R is a parallel combination of element H and a damping element described by a Mittag-Leffler fractional exponential

generic function in an integral form, formulated by Rabotnov [3]. Element S uses a fractional power generic function, as proposed by Schapery [4].

The H-S and modified H-S models were applied in [5-10]. Schapery's single integral constitutive model was formulated and tested. Elastic-viscoelastic-viscoplastic tensile creep tests on a polymer-matrix composite were conducted at three levels of temperature in [11]. The linear viscoelastic behaviour of selected polymers was discussed in [12], using the creep function as a sum of normal exponents. A concurrent micromechanical model for unidirectional fibre-reinforced polymer matrix (UFRP) composites was formulated in [13]. A transient compliance followed the Prony series exponential form.

The long-term linear viscoelastic behaviour of fibre-reinforced polymer matrix composites, with the fibre and matrix phases described by a four-parameter rheological law, was discussed in [14]. Prediction of the viscoelastic behaviour of UFRP composites was developed in [15]. The H-K viscoelastic model for the matrix was used. The creep rupture phenomenon of the unidirectional glass fibre-reinforced vinyl ester matrix composite rod subjected to a shear-traction load was investigated experimentally and numerically in [16]. A power law for the matrix creep function was assumed.

A linear viscoelastic model for unidirectional glass fibre-reinforced polymer matrix composites was formulated in [17]. The fibres were assumed to be elastic, and the matrix was described by the M-K viscoelastic model. The results from 42-month creep experiments in the fibre direction on a uniaxial E-glass fibre-reinforced epoxy matrix composite are presented in [18]. The viscoelastic models were taken from the literature, i.e. the Burgers, Findley, and Nutting models.

A three-dimensional temperature-dependent viscoelastic constitutive model for UFRP composites is developed in [19]. The integrity basis for the decomposition is used to formulate the energy functional, which enables uncoupled constitutive laws to be defined. A generalized Maxwell model is applied for the composite. Thermal strains and temperature effects on the viscoelastic behaviour are introduced by the time-temperature superposition principle.

The research presented in [5-19] can be summarized as follows: The viscoelastic and plastic behaviour of thermosets and UFRP composites was described by H-S, modified H-S, H-K, M-K, fractional M, generalized M, Leonov, Burgers, Findley, and Nutting rheological models. The viscoelastic modelling of UFRP composites is most often based directly on experimental creep or creep-recovery tests. A promising tool for modelling the viscoelasticity of thermosets is the time-temperature superposition principle. To date, the effect of ageing thermosets and UFRP composites on their long-term rheological behaviour has not been studied.

In Poland, research on the rheology of thermosetting polymers and UFRP composites has been ongoing since

1995 by Klasztorny et al. [20-28]. This research is a continuation of the research conducted by Prof. A.P. Wilczynski in the period 1965-1995. The H-R/H-R (shear/bulk approach) rheological models for thermosets and UFRP composites were formulated in [20, 21]. A UFRP composite was described by 27 viscoelastic constants determined numerically using a weakly conditional algorithm. In addition, after publication, the input data on the bulk creep of the exemplary thermoset turned out to be wrong. The M-R-K rheological model for thermosets and thermoplastics, described by 14 elastic/viscoelastic/viscous constants estimated numerically and tested on polyester, was developed in [22]. The H-R-2K rheological model for thermosets, described by 9 elastic/viscoelastic constants, was formulated in [23-25]. For UFRP composites, this approach results in 18 elastic/viscoelastic constants estimated numerically. The H-R-2K/H (shear/bulk approach) rheological model for thermosets, described by 8 elastic/viscoelastic constants, was formulated in [26, 27]. An analytical-numerical algorithm to simulate reversible rheological processes in thermosets was developed in [28].

The research presented in [20-28] can be summarized as follows. The H-R/H-R rheological model for thermosets is inadequate as it is based on incorrect viscoelastic bulk deformations. The M-R-K, H-R-2K, H-R-2K/H rheological models for thermosets are described by relatively large numbers of viscoelastic constants creating fuzzy sets. To date, only coupled standard constitutive equations of the rheology of UFRP composites have been formulated, which correspond to the H-R/H-R and H-R-2K rheological models of thermosets.

Further development of the analytical rheological modelling of thermosets and UFRP composites is presented by Klasztorny and Nycz in [2, 29]. New phenomenological rheological models coded as H-R/H were formulated, based on a Mittag-Leffler fractional exponential generic function in an integral form, the homogenization theory for UFRP composites with isotropic fibres and the viscoelastic-elastic correspondence principle (VECP). Compared to [2, 29], this study includes the following changes / extensions / corrections:

- formulation of the refined rheological modelling of thermosetting polymers and unidirectional monotropic fibre-reinforced thermoset matrix (UFRP) composites (H-R/H rheological models),
- simplification of the H-R/H rheological model of a UFRP composite by omitting the negligibly small viscoelastic strains corresponding to quasi-shear compliance  $S_{s1}(t)$ , which results in a reduced number of independent viscoelastic constants,
- formulation of the improved homogenization theory for monotropic fibres, based on [30], with the compatibility condition in the third Lamé-type task put on the radial displacements,
- experimental validation of the compatibility condition in the third Lamé-type task on the improved

reliability UFRT composites reported by Soden et al. [31, 32],

- experimental validation of the improved homogenization theory for monotropic fibres on the improved reliability UFRT composites reported by Soden et al. [31, 32],
- experimental identification of viscoelastic constants of the selected epoxy resin, corresponding to the H-R/H rheological model of a thermoset resin,
- numerical validation of the H-R/H rheological model of a UFRT composite on the improved reliability UFRT composites taken from [31, 32],
- adoption of a more natural system of designations,
- elimination of proof errors in the equations.

In the following sections, the improved rheological modelling of thermosets, the improved homogenization theory for UFRT composites with monotropic fibres, the improved analytical rheological modelling of UFRT composites, and the improved formulation of complementary problems will be presented in abbreviated versions compared to [2, 29]. The supplementary formulae are presented in Appendix A.

## IMPROVED ELASTIC AND RHEOLOGICAL MODELLING OF THERMOSETS

The considerations in this section are an abbreviated version of those presented in [2], adopting a more natural system of designations. The following assumptions, valid in fibre-reinforced plastic matrix (FRP) laminate shell structural design, are made for thermosets constituting FRP matrices:

- A thermoset is an isotropic material exhibiting linearly viscoelastic shear strains and linearly elastic bulk strains.
- A thermoset is a new (unaged) material, fully relaxed from the residual stresses induced by the manufacturing processes.
- Quasi-static long-term isothermal rheological processes under normal conditions (temperature 20°C, humidity 50%) are considered.
- Appropriately low levels of stresses and strains secure the reversibility of the rheological processes.

The stress and strain components in any Cartesian coordinate system  $x_1x_2x_3$  are denoted as follows:  $\sigma_1, \sigma_2, \sigma_3$  – normal stresses,  $\tau_{23}, \tau_{13}, \tau_{12}$  – shear stresses,  $\varepsilon_1, \varepsilon_2, \varepsilon_3$  – normal strains,  $\gamma_{23}, \gamma_{13}, \gamma_{12}$  – shear strains. A linearly elastic thermoset is considered, described by two independent elastic constants, i.e.  $E_m$  – Young's modulus,  $\nu_m$  – Poisson's ratio. The shear and bulk modules of a thermoset are dependent elastic constants, i.e.

$$G_m = E_m/2(1 + \nu_m), \quad B_m = E_m/3(1 - 2\nu_m) \quad (1)$$

Classic coupled standard constitutive equations of the linear elasticity of a thermoset may be written in the following matrix notation:

$$\boldsymbol{\varepsilon} = \mathbf{S}_e \boldsymbol{\sigma}, \quad \boldsymbol{\delta} = S_{se} \boldsymbol{\tau} \quad (2)$$

where:

$$\boldsymbol{\varepsilon} = \begin{bmatrix} \varepsilon_1 \\ \varepsilon_2 \\ \varepsilon_3 \end{bmatrix}, \quad \boldsymbol{\delta} = \begin{bmatrix} \delta_{23} \\ \delta_{13} \\ \delta_{12} \end{bmatrix}, \quad \boldsymbol{\sigma} = \begin{bmatrix} \sigma_1 \\ \sigma_2 \\ \sigma_3 \end{bmatrix}, \quad \boldsymbol{\tau} = \begin{bmatrix} \tau_{23} \\ \tau_{13} \\ \tau_{12} \end{bmatrix} \quad (3)$$

$$\mathbf{S}_e = \begin{bmatrix} S_{11e} & S_{12e} & S_{12e} \\ & S_{11e} & S_{12e} \\ \text{symm.} & & S_{11e} \end{bmatrix},$$

$$S_{11e} = 1/E_m, \quad S_{12e} = -\nu_m/E_m, \quad S_{se} = 1/2G_m$$

with  $\delta_{jk} = \gamma_{jk}/2, jk = 23, 13, 12$ . Vectors  $\boldsymbol{\varepsilon}, \boldsymbol{\delta}, \boldsymbol{\sigma}, \boldsymbol{\tau}$  represent parts of the strain and stress tensors at point  $(x_1, x_2, x_3)$ , i.e. normal strains, half shear strains, normal stresses, and shear stresses. Quantity  $\mathbf{S}_e$  is the elastic compliance matrix, while quantity  $S_{se}$  is the elastic shear compliance for a thermoset. Equation (2)<sub>1</sub> is coupled, whereas Eqn. (2)<sub>2</sub> is uncoupled.

By inverting Eqns. (2), classic coupled inverse constitutive equations of the linear elasticity of a thermoset are obtained, i.e.

$$\boldsymbol{\sigma} = \mathbf{C}_e \boldsymbol{\varepsilon}, \quad \boldsymbol{\tau} = C_{se} \boldsymbol{\delta} \quad (4)$$

where:

$$\mathbf{C}_e = \begin{bmatrix} C_{11e} & C_{12e} & C_{12e} \\ & C_{11e} & C_{12e} \\ \text{symm.} & & C_{11e} \end{bmatrix} \quad (5)$$

$$C_{11e} = E_m(1 - \nu_m^2)/\Delta, \quad C_{12e} = E_m(1 + \nu_m)\nu_m/\Delta$$

$$\Delta = 1 - 3\nu_m^2 - 2\nu_m^3, \quad C_{se} = 2G_m$$

Quantity  $\mathbf{C}_e$  is the elastic stiffness matrix, while quantity  $C_{se}$  is the elastic shear stiffness for a thermoset. Equation (4)<sub>1</sub> is coupled, whereas Eqn. (4)<sub>2</sub> is uncoupled.

Coupled Eqn. (2)<sub>1</sub> can be transformed into uncoupled standard constitute equations of the linear elasticity of a thermoset, i.e. (e.g. [22])

$$\boldsymbol{\varepsilon}_s = S_{se} \boldsymbol{\sigma}_s, \quad \varepsilon_b = S_{be} \sigma_b \quad (6)$$

where:

$$\boldsymbol{\varepsilon}_s = \begin{bmatrix} \varepsilon_1 - \varepsilon_b \\ \varepsilon_2 - \varepsilon_b \\ \varepsilon_3 - \varepsilon_b \end{bmatrix}, \quad \boldsymbol{\sigma}_s = \begin{bmatrix} \sigma_1 - \sigma_b \\ \sigma_2 - \sigma_b \\ \sigma_3 - \sigma_b \end{bmatrix} \quad (7)$$

$$\varepsilon_b = (\varepsilon_1 + \varepsilon_2 + \varepsilon_3)/3, \quad \sigma_b = (\sigma_1 + \sigma_2 + \sigma_3)/3, \quad S_{be} = 1/3B_m$$

Vectors  $\boldsymbol{\varepsilon}_s, \boldsymbol{\delta}, \boldsymbol{\sigma}_s, \boldsymbol{\tau}$  are the deviatoric parts of the strain and stress tensors of a thermoset at point  $(x_1, x_2, x_3)$ , accordingly. Quantities  $\varepsilon_b, \sigma_b$  are axiators of the strain and stress tensors of a thermoset, respectively. Coefficient  $S_{be}$  is the elastic bulk compliance.

By inverting Eqns. (6), uncoupled inverse constitutive equations of the linear elasticity of a thermoset are obtained, i.e.

$$\boldsymbol{\sigma}_s = C_{se} \boldsymbol{\varepsilon}_s, \quad \boldsymbol{\sigma}_b = C_{be} \boldsymbol{\varepsilon}_b \quad (8)$$

where  $C_{be} = 3B_m$  is the elastic bulk stiffness.

The following relationships are obtained from Eqns. (2)-(8):

$$\mathbf{S}_e = S_{se} (\mathbf{I} - \mathbf{A}) + S_{be} \mathbf{A},$$

$$\begin{aligned} \mathbf{C}_e &= C_{se} (\mathbf{I} - \mathbf{A}) + C_{be} \mathbf{A} \\ \mathbf{I} &= \text{diag}(1, 1, 1), \quad \mathbf{A} = \frac{1}{3} \begin{bmatrix} 1 & 1 & 1 \\ 1 & 1 & 1 \\ 1 & 1 & 1 \end{bmatrix} \end{aligned} \quad (9)$$

where:  $\mathbf{I}, \mathbf{A}$  – transformation matrices.

Uncoupled standard constitutive equations of the linear rheology of a thermoset, corresponding to Eqns. (6), (2)<sub>2</sub>, have the following form:

$$\begin{aligned} \boldsymbol{\varepsilon}_s(t) &= S_s(t) \otimes \boldsymbol{\sigma}_s(t), \quad \boldsymbol{\varepsilon}_b(t) = S_{be} \boldsymbol{\sigma}_b(t), \\ \boldsymbol{\delta}(t) &= S_s(t) \otimes \boldsymbol{\tau}(t) \end{aligned} \quad (10)$$

for time  $t \geq 0$ , with

$$\begin{aligned} S_s(t) &= S_{se} \left[ 1 + c \int_0^t \Phi(v) dv \right], \\ \Phi(t) &= \frac{1}{T_c} \int_0^\infty \exp\left(-\frac{ut}{T_c}\right) u L(u) du \\ L(u) &= \frac{\sin \pi r}{\pi u} \frac{u^r}{1 + 2u^r \cos \pi r + u^{2r}}, \\ 0 &< r < 1 \end{aligned} \quad (11)$$

The following nomenclature is introduced:  $L(u)$  – function defining a Mittag-Leffler fractional exponential function in an integral form,  $r$  – fraction defining a Mittag-Leffler fractional exponential function in an integral form,  $T_c$  – retardation time,  $\Phi(t)$  – Mittag-Leffler fractional exponential generic function in an integral form for shear stresses,  $S_s(t)$  – elastic-viscoelastic shear compliance,  $c$  – long-term creep coefficient,  $\otimes$  – convolution product operator.

A linear rheological model described by Eqns. (10)-(11) is denoted as H-R/H. Under the assumptions made, a thermoset is described by two independent elastic constants ( $E_m, \nu_m$ ) and three independent viscoelastic constants ( $T_c, r, c$ ). A mechanical representation of the H-R/H model consists of a Hooke elastic element and a Rabotnov viscoelastic element (connected in a series) for the strain deviator and a Hooke elastic element for the strain axiator. For boundary value  $r = 1$ , the H-R/H fractional model transforms into the H-K/H standard model (see Appendix A).

Consider the pure shear creep of a thermoset, induced by stresses

$$\boldsymbol{\sigma}_s(t) = \boldsymbol{\sigma}_{s0} H(t), \quad \boldsymbol{\tau}(t) = \boldsymbol{\tau}_0 H(t) \quad (12)$$

where:  $\boldsymbol{\sigma}_{s0}, \boldsymbol{\tau}_0$  – constant shear stresses,  $H(t)$  – Heaviside function. Equations (10)<sub>1</sub>, (10)<sub>3</sub> result in

$$\begin{aligned} \boldsymbol{\varepsilon}_s(t) &= S_{se} [1 + c \varphi(t)] \boldsymbol{\sigma}_{s0}, \\ \boldsymbol{\delta}(t) &= S_{se} [1 + c \varphi(t)] \boldsymbol{\tau}_0 \end{aligned} \quad (13)$$

where:

$$\varphi(t) = \int_0^t \Phi(v) dv = 1 - \int_0^\infty \exp\left(-\frac{ut}{T_c}\right) L(u) du \quad (14)$$

is the creep function.

The Laplace transforms made on Eqns. (10)<sub>1</sub>, (10)<sub>3</sub> have the form:

$$\begin{aligned} \bar{\boldsymbol{\varepsilon}}_s(q) &= S_{se} [1 + c \bar{\Phi}(q)] \bar{\boldsymbol{\sigma}}_s(q), \\ \bar{\boldsymbol{\delta}}(q) &= S_{se} [1 + c \bar{\Phi}(q)] \bar{\boldsymbol{\tau}}(q) \end{aligned} \quad (15)$$

where  $q$  – a complex variable, and

$$\begin{aligned} \bar{\boldsymbol{\varepsilon}}_s(q) &= \int_0^\infty \exp(-qt) \boldsymbol{\varepsilon}_s(t) dt, \\ \bar{\boldsymbol{\sigma}}_s(q) &= \int_0^\infty \exp(-qt) \boldsymbol{\sigma}_s(t) dt \\ \bar{\boldsymbol{\delta}}(q) &= \int_0^\infty \exp(-qt) \boldsymbol{\delta}(t) dt, \\ \bar{\boldsymbol{\tau}}(q) &= \int_0^\infty \exp(-qt) \boldsymbol{\tau}(t) dt \\ \bar{\Phi}(q) &= \int_0^\infty \exp(-qt) \Phi(t) dt = \frac{1}{1 + (qT_c)^r} \end{aligned} \quad (16)$$

For the harmonic stress programmes

$$\boldsymbol{\sigma}_s^*(t) = \boldsymbol{\sigma}_{s0} \exp(i\omega t), \quad \boldsymbol{\tau}^*(t) = \boldsymbol{\tau}_0 \exp(i\omega t) \quad (17)$$

where:  $\boldsymbol{\sigma}_{s0}, \boldsymbol{\tau}_0$  – shear stress amplitudes. The elastic-viscoelastic responses obtained from Eqns. (10)<sub>1</sub>, (10)<sub>3</sub> are (evidence included in [2])

$$\begin{aligned} \boldsymbol{\varepsilon}_s^*(t) &= S_{se} \left[ 1 + c \int_0^t \exp(-i\omega v) \Phi(v) dv \right] \boldsymbol{\sigma}_s^*(t) \\ \boldsymbol{\delta}^*(t) &= S_{se} \left[ 1 + c \int_0^t \exp(-i\omega v) \Phi(v) dv \right] \boldsymbol{\tau}^*(t) \end{aligned} \quad (18)$$

where:  $i = \sqrt{-1}$  is an imaginary unit,  $( )^*$  denotes a complex quantity, and  $\omega > 0$  is a circular frequency. The steady-state harmonic responses are obtained by putting  $t \rightarrow \infty$  in Eqns. (18), i.e.

$$\boldsymbol{\varepsilon}_s^*(t) = S_s^*(\omega) \boldsymbol{\sigma}_s^*(t), \quad \boldsymbol{\delta}^*(t) = S_s^*(\omega) \boldsymbol{\tau}^*(t) \quad (19)$$

where:

$$\begin{aligned} S_s^*(\omega) &= S_{se} [1 + c \bar{\Phi}(i\omega)] = S_s'(\omega) + iS_s''(\omega) \\ S_s'(\omega) &= S_{se} \left[ 1 + c \frac{1 + (\omega T_c)^r \cos(\pi r/2)}{1 + 2(\omega T_c)^r \cos(\pi r/2) + (\omega T_c)^{2r}} \right] \\ S_s''(\omega) &= -S_{se} c \frac{(\omega T_c)^r \sin(\pi r/2)}{1 + 2(\omega T_c)^r \cos(\pi r/2) + (\omega T_c)^{2r}} \end{aligned} \quad (20)$$

with:  $S_s^*(\omega)$  – complex shear compliance,  $S_s'(\omega)$  – shear storage compliance,  $S_s''(\omega)$  – shear loss compliance.

Inverting Eqns. (15) yields (evidence included in [2])

$$\begin{aligned}\bar{\sigma}_s(q) &= C_{se}[1 - d \bar{\Psi}(q)]\bar{\epsilon}_s(q), \\ \delta(q) &= C_{se}[1 - d \bar{\Psi}(q)]\bar{\tau}(q)\end{aligned}\quad (21)$$

where:

$$d = \frac{c}{1+c}, \quad \bar{\Psi}(q) = \frac{1}{1+(qT_d)^r}, \quad T_d^r = \frac{1}{1+c}T_c^r \quad (22)$$

with:  $T_d$  – relaxation time,  $\Psi(t)$  – Mittag-Leffler fractional exponential generic function in an integral form for shear strains,  $\bar{\Psi}(q)$  – Laplace transform on  $\Psi(t)$ ,  $d$  – long-term relaxation coefficient. Relaxation constants  $d, T_d$  are expressed in terms of independent creep constants  $c, T_c$ . In practice, constant  $T_d$  is calculated from the equivalent formula

$$T_d = T_c \exp\left(\frac{1}{r} \ln \frac{1}{1+c}\right) \quad (23)$$

By applying the inverse Laplace transform on Eqns. (21) and taking into account Eqn. (10)<sub>2</sub>, uncoupled inverse constitutive equations of the linear rheology of a thermoset are obtained, i.e.

$$\begin{aligned}\sigma_s(t) &= C_s(t) \otimes \epsilon_s(t), \quad \sigma_b(t) = C_{be} \epsilon_b(t), \\ \tau(t) &= C_s(t) \otimes \delta(t)\end{aligned}\quad (24)$$

where:

$$\begin{aligned}C_s(t) &= C_{se} \left[ 1 - d \int_0^t \Psi(v) dv \right], \\ \Psi(t) &= \frac{1}{T_d} \int_0^\infty \exp\left(-\frac{ut}{T_d}\right) u L(u) du\end{aligned}\quad (25)$$

with  $C_s(t)$  – elastic-viscoelastic shear stiffness. Generic functions  $\Phi(t), \Psi(t)$  have analogous properties, as specified for  $\Phi(t)$  in Appendix A.

Consider the pure shear relaxation of a thermoset induced by strains

$$\epsilon_s(t) = \epsilon_{s0} H(t), \quad \delta(t) = \delta_0 H(t) \quad (26)$$

where:  $\epsilon_{s0}, \delta_0$  – constant shear strains. Equations (24)<sub>1</sub>, (24)<sub>3</sub> result in

$$\begin{aligned}\sigma_s(t) &= C_{se} [1 - d \psi(t)] \epsilon_{s0}, \\ \tau(t) &= C_{se} [1 - d \psi(t)] \delta_0\end{aligned}\quad (27)$$

where the relaxation function is expressed as

$$\begin{aligned}\psi(t) &= \int_0^t \Psi(v) dv \\ &= 1 - \int_0^\infty \exp\left(-\frac{ut}{T_d}\right) L(u) du\end{aligned}\quad (28)$$

Coupled standard/inverse constitutive equations of the linear rheology of a thermoset result from Eqns. (2, 4, 6, 8-10, 24) and have the following final form:

$$\begin{aligned}\epsilon(t) &= \mathbf{S}(t) \otimes \sigma(t), \quad \delta(t) = S_s(t) \otimes \tau(t) \\ \sigma(t) &= \mathbf{C}(t) \otimes \epsilon(t), \quad \tau(t) = C_s(t) \otimes \delta(t)\end{aligned}\quad (29)$$

where:

$$\begin{aligned}\mathbf{S}(t) &= S_s(t) (\mathbf{I} - \mathbf{A}) + S_{be} \mathbf{A}, \\ \mathbf{C}(t) &= C_s(t) (\mathbf{I} - \mathbf{A}) + C_{be} \mathbf{A}\end{aligned}\quad (30)$$

are the elastic-viscoelastic compliance and stiffness matrices for a thermoset. Based on Eqns. (11)<sub>1</sub>, (25)<sub>1</sub>, Eqns. (29) can be rewritten in the following explicit form:

a) standard equations:

$$\begin{aligned}\epsilon(t) &= \mathbf{S}_e \sigma(t) + S_{se} c \int_0^t \Phi(v) dv (\mathbf{I} - \mathbf{A}) \otimes \sigma(t) \\ \delta(t) &= S_{se} \tau(t) + S_{se} c \int_0^t \Phi(v) dv \otimes \tau(t)\end{aligned}\quad (31)$$

b) inverse equations:

$$\begin{aligned}\sigma(t) &= \mathbf{C}_e \epsilon(t) - C_{se} d \int_0^t \Psi(v) dv (\mathbf{I} - \mathbf{A}) \otimes \epsilon(t) \\ \tau(t) &= C_{se} \delta(t) - C_{se} d \int_0^t \Psi(v) dv \otimes \delta(t)\end{aligned}\quad (32)$$

## IMPROVED HOMOGENIZATION THEORY OF UFRP COMPOSITE

This Section formulates an improved quasi-exact homogenization theory of a UFRP composite. The theory is based on [30]. Compared to this reference, the following changes / extensions / corrections were made:

- assumption that the reciprocal Maxwell relations are compatible with CAE systems (MSC.Marc, LS-Dyna etc.),
- adoption of the compatibility condition in the third Lamé-type task imposed on the radial displacements of the representative volume cell (RVC),
- experimental validation of the compatibility condition in the third Lamé-type task on improved reliability UFRT composites taken from [31],
- adoption of a more natural system of designations,
- elimination of proof errors in the equations.

The complete analytical homogenization theory regarding RVC is presented in [30]; hence, in this study a shortened version of an improved theory will be presented.

The following assumptions are made in reference to the UFRP homogenization theory:

- A UFRP composite consists of two components, the matrix and the fibre.
- The matrix is a linearly elastic isotropic solid body.
- The fibre is a linearly elastic monotropic solid body with the direction of monotropy coinciding with the fibre direction.
- The fibres have an identical circular cross-section.
- The fibres are perfectly bonded to the matrix; the interphase is neglectable.

- The fibres are long, rectilinear, arranged unidirectionally and uniformly in the matrix in a hexagonal scheme.
- The cylindrical RVC is volume-equivalent to the actual hexagonal RVC.
- The homogenized UFRP composite is a monotropic solid body with the direction of monotropy coinciding with the fibre direction.
- Mass forces vanish.

RVC extracted from a UFRP composite is a cylinder consisting of a circular central disc modelling the fibre section and a ring disc modelling the matrix section surrounding the fibre, as shown in [29]. The central disc is of radius  $a$  and thickness  $2h$  and the ring disc is of outer radius  $b$  and thickness  $2h$ , whereby  $a = b\sqrt{f}$ , where  $f$  is the real fibre volume fraction. The homogenized RVC is a circular disc with radius  $b$  and thickness  $2h$ . RVC is described in the  $x_1r\varphi$  cylindrical coordinate system corresponding to the  $x_1x_2x_3$  Cartesian coordinate system ( $x_1$  – fibre axis,  $x_2x_3$  – transverse isotropy plane). Note that RVC is a  $2h$  thick section of an infinitely long two-phase cylinder.

The constituents and the homogenized UFRP composite are described by the following independent elastic constants:

- isotropic matrix:  $E_m, \nu_m$ ,
- monotropic fibre:  $E_{1f}$  – longitudinal Young's modulus,  $E_{2f}$  – transverse Young's modulus,  $\nu_{12f}$  – major Poisson's ratio in the  $x_1x_2$  plane,  $\nu_{23f}$  – Poisson's ratio in the  $x_2x_3$  plane,  $G_{12f}$  – shear modulus in the  $x_1x_2$  plane,
- effective elastic constants (EECs) of the monotropic homogenized UFRP composite:  $E_1$  – longitudinal Young's modulus,  $E_2$  – transverse Young's modulus,  $\nu_{12}$  – major Poisson's ratio in the  $x_1x_2$  plane,  $\nu_{23}$  – Poisson's ratio in the  $x_2x_3$  plane,  $G_{12}$  – shear modulus in the  $x_1x_2$  plane.

The reciprocal Maxwell relations concerning the fibre and the homogenized composite, adopted in CAE systems, are of the form

$$\nu_{jkf}/E_{jf} = \nu_{kjf}/E_{kf}, \quad \nu_{jk}/E_j = \nu_{kj}/E_k, \quad j, k = 1, 2, 3 \quad (33)$$

Other EECs describing a fibre and a UFRP composite ( $E_{3f}, \nu_{13f}, G_{13f}, G_{23f}, \nu_{21f}, \nu_{32f}, \nu_{31f}, E_3, \nu_{13}, \nu_{31f}, E_3, \nu_{13}, G_{13}, G_{23}, \nu_{21}, \nu_{32}, \nu_{31}$ ) are determined from the transverse isotropy conditions and from Eqns. (33).

The EECs of the homogenized UFRP composite will be determined analytically from the compatibility conditions put on the solutions before and after the homogenization of appropriately chosen tasks of the theory of linear elasticity (Lamé-type tasks).

Based on Eqns. (3)<sub>5-8</sub>, (7)<sub>5</sub>, (9)<sub>1,3</sub>, the elastic directional compliances of a plastic matrix are expressed in terms of the elastic shear/bulk compliances of the matrix, i.e.

$$S_{11e} = (2S_{se} + S_{be})/3, \quad S_{12e} = (S_{be} - S_{se})/3 \quad (34)$$

where (see Eqns. (3)<sub>8</sub>, (7)<sub>5</sub>):

$$S_s = 1/2G_m, \quad S_b = 1/3B_m \quad (35)$$

with the shear and bulk matrix modules defined by Eqns. (1). By multiplying Eqn. (34) by  $E_{1f}$ , the following dimensionless relationships are obtained:

$$s_{11} = (2s_s + s_b)/3, \quad s_{12} = (s_b - s_s)/3 \quad (36)$$

where:

$$\begin{aligned} s_{11} &= E_{1f}/E_m, \quad s_{12} = -\nu_m E_{1f}/E_m, \\ s_s &= E_{1f}/2G_m, \quad s_b = E_{1f}/3B_m \end{aligned} \quad (37)$$

The following factor equivalent to the selected reciprocal Maxwell relation is defined

$$\kappa = \nu_{21f}/\nu_{12f} = E_{2f}/E_{1f} \quad (38)$$

In further considerations, quantities

$$\begin{aligned} S_{11e} &= 1/E_1, \quad S_{22e} = 1/E_2, \\ S_{12e} &= -\nu_{12}/E_1, \quad S_{23e} = -\nu_{23}/E_2 \\ S_{s23e} &= 1/2G_{23} = (1 + \nu_{23})/E_2 = S_{22e} - S_{23e}, \\ S_{s12e} &= 1/2G_{12} \end{aligned} \quad (39)$$

are elements of elastic compliance matrices  $\mathbf{S}_e, \mathbf{S}_{se}$  of the homogeneous monotropic composite, formulated in this study.

The same quantities  $S_{11h}, S_{22h}, S_{12h}, S_{23h}, S_{s23h}, S_{s12h}$  will be determined from the refined homogenization theory. Compliances

$$S_{2h} = (1 - \nu_{23})/E_2, \quad S_{s23h} = (1 + \nu_{23})/E_2 \quad (40)$$

allow two compliances to be determined, i.e.

$$S_{22h} = (S_{2h} + S_{s23h})/2, \quad S_{23h} = (S_{2h} - S_{s23h})/2 \quad (41)$$

The following quantities corresponding to RVC are introduced:

$A, B, C, D$  – integration constants corresponding to the matrix,

$A_f, B_f, C_f$  – integration constants corresponding to the fibre,

$u_{1m}, u_m, v_m$  – displacement components in cylindrical coordinates, corresponding to the matrix,

$u_{1f}, u_f, v_f$  – displacement components in cylindrical coordinates, corresponding to the fibre,

$u_1, u, v$  – displacement components in cylindrical coordinates, corresponding to the homogenized composite,

$\sigma_{1m}, \sigma_{rm}, \sigma_{\varphi m}, \tau_{r\varphi m}, \tau_{1rm}$  – stress components in cylindrical coordinates, corresponding to the matrix,

$\sigma_{1f}, \sigma_{rf}, \sigma_{\varphi f}, \tau_{r\varphi f}, \tau_{1rf}$  – stress components in cylindrical coordinates, corresponding to the fibre,

$\sigma_1, \sigma_r, \sigma_\varphi, \tau_{r\varphi}, \tau_{1r}$  – stress components in cylindrical coordinates, corresponding to the homogenized composite,

$\sigma_0, \tau_0$  – maximum of a selected normal/shear stress,

$p_{11}, p_{22}, p_{12}, p_{21}, p_1, p_2, p_3, p_4, p$  – auxiliary coefficients.

The displacement and stress components in the  $x_1 r \varphi$  coordinate system, corresponding to the homogenized RVC, were illustrated in [29].

The following Lamé-type tasks of the theory of linear elasticity, referred to RVC before and after homogenization, were chosen: 1) longitudinal uniform tension in the  $x_1$  direction; 2) axially-symmetric transverse tension in the  $x_2 x_3$  plane; 3) transverse shear in the  $x_2 x_3$  plane; 4) longitudinal shear in the  $x_1 x_2$  plane. These tasks are illustrated in [29].

Consider the first Lamé-type task. The longitudinal elongation of both phases  $u_1 = \text{const}$ ; hence, the normal stress distribution before homogenization  $\sigma_{1m} = \text{const}$ ,  $\sigma_{1f} = \text{const}$  and after homogenization  $\sigma_0 = \text{const}$ . The general solutions are of the form (evidence included in [30]):

– stresses and displacements corresponding to the fibre ( $0 \leq r \leq a$ ):

$$\begin{aligned} \sigma_{rf} &= 2C_f, \quad \sigma_{\varphi f} = 2C_f \\ u_f(r) &= r[2(1 - \nu_{23f})C_f - \nu_{21f}\sigma_{1f}]/E_{2f} \\ u_{1f}(x_1) &= x_1(\sigma_{1f} - 4\nu_{12f}C_f)/E_{1f} \end{aligned} \quad (42)$$

– stresses and displacements corresponding to the matrix ( $a \leq r \leq b$ ):

$$\begin{aligned} \sigma_{rm}(r) &= A/r^2 + 2C, \quad \sigma_{\varphi m}(r) = -A/r^2 + 2C \\ u_m(r) &= r[-\nu_m\sigma_{1m} - (1 + \nu_m)A/r^2 + 2(1 - \nu_m)C]/E_r \\ u_{1m}(x_1) &= x_1(\sigma_{1m} - 4\nu_m C)/E_m \end{aligned} \quad (43)$$

– stresses and displacements corresponding to the homogenized RVC ( $0 \leq r \leq b$ ):

$$\begin{aligned} \sigma_r &= 0, \quad \sigma_\varphi = 0 \\ u(r) &= -r\nu_{12}\sigma_0/E_1, \quad u_1(x_1) = x_1\sigma_0/E_1 \end{aligned} \quad (44)$$

The stress boundary conditions have the form

$$\sigma_{1f}f + \sigma_{1m}(1 - f) = \sigma_0, \quad \sigma_{rm}(b) = 0 \quad (45)$$

The continuity conditions are of the form

$$\begin{aligned} \sigma_{rf}(a) &= \sigma_{rm}(a), \quad u_f(a) = u_m(a), \\ u_{1f}(h) &= u_{1m}(h) \end{aligned} \quad (46)$$

The displacement compatibility conditions have the form

$$u_m(b) = u(b), \quad u_{1m}(h) = u_1(h) \quad (47)$$

Equations (45)-(47) form a system of seven linear algebraic equations with unknowns  $\sigma_{1f}, \sigma_{1m}, C_f, A, C, S_{11h}, S_{12h}$ . The results in terms of the elastic compliances of the homogenized composite are as follows:

$$\begin{aligned} S_{11h} &= (p_2s_{11} - 2p_1s_{12})/p/E_{1f}, \\ S_{12h} &= (p_2s_{12} - 2p_1s_{11})/p/E_{1f} \end{aligned} \quad (48)$$

where:

$$\begin{aligned} p_1 &= p_{22}\nu_{21f} - p_{12}, \quad p_2 = p_{11} - p_{21}\nu_{21f}, \\ p &= p_{11}p_{22} - p_{12}p_{21} \\ p_{11} &= (1 - f)(1 - \nu_{23f}) + \\ &+ (1 + f)s_{11}\kappa - (1 - f)s_{12}\kappa, \\ p_{22} &= 1 + f(s_{11} - 1) \\ p_{12} &= (1 - f)\nu_{21f} - fs_{12}\kappa, \\ p_{21} &= 2(1 - f)\nu_{12f} - 2fs_{12} \end{aligned} \quad (49)$$

Consider the second Lamé-type task. The longitudinal contraction (negative elongation) of both phases  $u_1 = \text{const}$ ; therefore, the normal stress distribution before homogenization  $\sigma_{1m} = \text{const}$ ,  $\sigma_{1f} = \text{const}$  and after homogenization  $\sigma_1 = 0$ . The stresses and displacements corresponding to the fibre and the matrix are described by Eqns. (42), (43), whereas for the homogenized RVC the results are of the form ( $0 \leq r \leq b$ ) (evidence included in [30]):

$$\begin{aligned} \sigma_r &= \sigma_0, \quad \sigma_\varphi = \sigma_0 \\ u(r) &= r(1 - \nu_{23})\sigma_0/E_2, \quad u_1(x_1) = -2x_1\nu_{12}\sigma_0/E_1 \end{aligned} \quad (50)$$

The stress boundary conditions have the form:

$$\sigma_{1f}f + \sigma_{1m}(1 - f) = 0, \quad \sigma_{rm}(b) = \sigma_0 \quad (51)$$

The continuity and compatibility conditions are described by Eqns. (46), (47). Equations (46), (47) and (51) form a system of seven linear algebraic equations with unknowns  $\sigma_{1f}, \sigma_{1m}, C_f, A, C, S_{2h}, S_{12h}$ . The results in terms of the elastic compliances of the homogenized UFRP composite have the form:

$$\begin{aligned} S_{2h} &= [s_{11} + s_{12} + (p_4s_{12} - 2p_3s_{11})/p]/E_{1f} \\ S_{12h} &= [s_{12} + (p_4s_{11}/2 - p_3s_{12})/p]/E_{1f} \end{aligned} \quad (52)$$

where

$$\begin{aligned} p_3 &= fp_{22}[(1 - \nu_m)s_{11}\kappa - (1 - \nu_{23f})] + \\ &+ 2fp_{12}(\nu_{12f} + s_{12}) \\ p_4 &= -2fp_{11}(\nu_{12f} + s_{12}) + \\ &- fp_{21}[(1 - \nu_m)s_{11}\kappa - (1 - \nu_{23f})] \end{aligned} \quad (53)$$

Coefficients  $p_{11}, p_{22}, p_{12}, p_{21}, p$  are defined in Eqns (49)<sub>3-7</sub>. It was proved that Eqns. (48)<sub>2</sub>, (52)<sub>2</sub> are equivalent.

Consider the third Lamé-type task related to the RVC loaded transversely on boundary  $r = b$  with the stresses:

$$\sigma_{rm}(b, \varphi) = \sigma_0 \cos 2\varphi, \quad \tau_{r\varphi m}(b, \varphi) = -\sigma_0 \sin 2\varphi \quad (54)$$

This load induces a planar strain state ( $\varepsilon_1 = 0$ ); thus, non-uniform normal stresses before and after

homogenization. The general solutions of this task have the following form (evidence included in [30]):

- stresses and displacements corresponding to the fibre ( $0 \leq r \leq a$ ):

$$\begin{aligned}\sigma_{rf}(\varphi) &= -2A_f \cos 2\varphi, \\ \sigma_{\varphi f}(r, \varphi) &= 2(A_f + 6B_f r^2) \cos 2\varphi \\ \tau_{r\varphi f}(r, \varphi) &= 2(A_f + 3B_f r^2) \sin 2\varphi \\ u_f(r, \varphi) &= \\ &= -2r[(1 + \nu_{23f})A_f + 2(\nu_{23f} + \nu_{21f}\nu_{12f})B_f r^2]/ \\ &E_{2f} \cdot \cos 2\varphi \\ v_f(r, \varphi) &= \\ &= 2r[(1 + \nu_{23f})A_f + (3 + \nu_{23f} - 2\nu_{21f}\nu_{12f})B_f r^2]/ \\ &E_{2f} \cdot \sin 2\varphi\end{aligned}\quad (55)$$

- stresses and displacements corresponding to the matrix ( $a \leq r \leq b$ ):

$$\begin{aligned}\sigma_{rm}(r, \varphi) &= -2(A + 3C/r^4 + 2D/r^2) \cos 2\varphi \\ \sigma_{\varphi m}(r, \varphi) &= 2(A + 6Br^2 + 3C/r^4) \cos 2\varphi \\ \tau_{r\varphi m}(r, \varphi) &= 2(A + 3Br^2 - 3C/r^4 - D/r^2) \sin 2\varphi \\ u_m(r, \varphi) &= -2r(1 + \nu_m) \cdot \\ &[A + 2\nu_m Br^2 - C/r^4 - 2(1 - \nu_m)D/r^2]/E_m \cdot \cos 2\varphi \\ v_m(r, \varphi) &= 2r[(1 + \nu_m)A + (3 + \nu_m - 2\nu_m^2)B r^2 + \\ &+ (1 + \nu_m)C/r^4 - (1 - \nu_m - 2\nu_m^2)D/r^2]/E_m \cdot \sin 2\varphi\end{aligned}\quad (56)$$

- stresses and displacements corresponding to the homogenized RVC ( $0 \leq r \leq b$ ):

$$\begin{aligned}\sigma_r(\varphi) &= \sigma_0 \cos 2\varphi, \\ \sigma_\varphi(\varphi) &= -\sigma_0 \cos 2\varphi, \\ \tau_{r\varphi}(\varphi) &= -\sigma_0 \sin 2\varphi \\ u(r, \varphi) &= r(1 + \nu_{23})\sigma_0/E_2 \cdot \cos 2\varphi \\ v(r, \varphi) &= -r(1 + \nu_{23})\sigma_0/E_2 \cdot \sin 2\varphi\end{aligned}\quad (57)$$

The stress boundary conditions are defined by Eqns. (54). The continuity conditions have the form:

$$\begin{aligned}\sigma_{rf}(a, \varphi) &= \sigma_{rm}(a, \varphi), \quad \tau_{r\varphi f}(a, \varphi) = \tau_{r\varphi m}(a, \varphi) \\ u_f(a, \varphi) &= u_m(a, \varphi), \quad v_f(a, \varphi) = v_m(a, \varphi)\end{aligned}\quad (58)$$

For the radial direction, the compatibility condition has the form

$$u_m(b, \varphi) = u(b, \varphi) \quad (59)$$

and for the circumferential direction

$$v_m(b, \varphi) = v(b, \varphi) \quad (60)$$

Previously, the compatibility condition in the third Lamé-type task was used in the form of Eqn. (59) or (60) or a linear combination resulting from these equations was applied [29, 33, 34, 30]. However, the experimental values of constants  $E_2, \nu_{23}$  used in the validation of a compatibility condition were uncertain (unverified by an independent laboratory). Moreover, the compatibility condition in [35] was local and did not take into account displacement errors. Therefore, the

choice of compatibility condition in the third Lamé-type task is still unadjusted.

Enhanced reliability experimental data for UFRP composites that can be used to validate experimentally the homogenization theory presented in this study were reported by Soden et al. [31, 32]. Four UFRP composites were considered in these references, i.e. EGG/LHD ( $f = 0.62$ ), EGS/MHD ( $f = 0.60$ ), AS4/3501-6 ( $f = 0.60$ ), T300/BSL ( $f = 0.60$ ), whereby:

- EGG = long E-glass fibre, 21xK43, Gevetex
  - EGS = long E-glass fibre, 1200tex, Silenka
  - AS4 = AS4 carbon fibre
  - T300 = T300 carbon fibre
- and
- LHD = LY556/HT907/DY063 epoxy, Ciba-Geigy
  - MHD = MY750/HY917/DY063 epoxy, Ciba-Geigy
  - 3501-6 = 3501-6 epoxy, Hercules
  - BSL = BSL914C epoxy, Ciba-Geigy.

The elastic constants of the constituents provided in [31, 32] are:

- EGG:  $E_{1f} = E_{2f} = 80$  GPa,  $\nu_{12f} = \nu_{23f} = 0.2$ ,  $G_{12f} = 33.33$  GPa
  - EGS:  $E_{1f} = E_{2f} = 74$  GPa,  $\nu_{12f} = \nu_{23f} = 0.2$ ,  $G_{12f} = 30.83$  GPa
  - AS4:  $E_{1f} = 225$  GPa,  $E_{2f} = 15$  GPa,  $\nu_{12f} = 0.2$ ,  $\nu_{23f} = 0.0714$ ,  $G_{12f} = 15$  GPa
  - T300:  $E_{1f} = 230$  GPa,  $E_{2f} = 15$  GPa,  $\nu_{12f} = 0.2$ ,  $\nu_{23f} = 0.0714$ ,  $G_{12f} = 15$  GPa
- and
- LHD, MHD:  $E_m = 3.35$  GPa,  $\nu_m = 0.35$
  - 3501-6:  $E_m = 4.2$  GPa,  $\nu_m = 0.34$
  - BSL:  $E_m = 4.0$  GPa,  $\nu_m = 0.35$ .

In this study, the EGG/LHD and EGS/MHD composites were used to validate experimentally a compatibility condition in the third Lamé-type task. Table 1 summarizes the predicted values of elastic constants  $E_2, \nu_{23}$  corresponding to a compatibility condition in the form of Eqn. (59) or Eqn. (60). The software developed in [29] was employed for the prediction. The experimental methods used to determine the elastic constants of the analysed UFRP composites or any arbitrary choice of the selected elastic constants are described in [32]. The experimental value of modulus  $E_2$  is of high reliability, while the experimental value of Poisson's ratio  $\nu_{23}$  seems to be arbitrary and overestimated. Due to the large values of the fibre volume fraction, the values of  $\nu_{23}, \nu_{23f}$  should be close to each other.

TABLE 1. Experimental and predicted values of elastic constants  $E_2, \nu_{23}$  for selected UFRP composites

| UFRP    | EEC        | Exp. [32] | Eqn. (59) | Eqn. (60) |
|---------|------------|-----------|-----------|-----------|
| EGG/LHD | $E_2$      | 17.7      | 16.7      | 7.49      |
|         | $\nu_{23}$ | 0.4       | 0.202     | 0.639     |
| EGS/MHD | $E_2$      | 16.2      | 15.5      | 7.09      |
|         | $\nu_{23}$ | 0.4       | 0.212     | 0.637     |

By comparing the predicted values with the experimental ones, it can be concluded that the compatibility condition imposed on the radial displacements is appropriate to determine constants  $E_2, \nu_{23}$ . The compatibility condition imposed on the circumferential displacements leads to the underestimation of modulus  $E_2$  and overestimation of Poisson's ratio  $\nu_{23}$ . The linear combination lowers the prediction accuracy and should therefore not be used.

Equations (54), (58), (59) form a system of seven linear algebraic equations with unknowns  $A_f, B_f, A, B, C, D, S_{s23h}$ . The result on another elastic compliance of the homogenized UFRP composite is

$$S_{s23h} = [1 + 4(1 - \nu_m) p_1/p](s_{11} - s_{12})/E_{1f} \quad (61)$$

where

$$p_1 = [1 + \nu_{23f} - (1 + \nu_m)s_{11}\kappa](p_{11} + p_{22} - p_{12} - p_{21})$$

$$p = p_{11}p_{22} - p_{12}p_{21} \quad (62)$$

with

$$p_{11} = 3(1 + \nu_{23f})(1/f^2 - 1) + 4(\nu_{23f} + \nu_{12f}\nu_{21f})(f - 1/f^2) + (1 + \nu_m)(3 - 4\nu_m f + 1/f^2)s_{11}\kappa$$

$$p_{22} = 2(1 + \nu_{23f})(1/f - 1) + (3 + \nu_{23f} - 2\nu_{12f}\nu_{21f})(f - 1/f) + [2(1 + \nu_m) - (3 + \nu_m - 2\nu_m^2)f + (1 - \nu_m - 2\nu_m^2)/f]s_{11}\kappa \quad (63)$$

$$p_{12} = 2(1 + \nu_{23f})(1/f - 1) + 2(\nu_{23f} + \nu_{12f}\nu_{21f})(f - 1/f) + 2(1 + \nu_m)[1 - \nu_m f + (1 - \nu_m)/f]s_{11}\kappa$$

$$p_{21} = 3(1 + \nu_{23f})(1/f^2 - 1) + 2(3 + \nu_{23f} - 2\nu_{12f}\nu_{21f})(f - 1/f^2) + [3(1 + \nu_m) - 2(3 + \nu_m - 2\nu_m^2)f - (1 + \nu_m)/f^2]s_{11}\kappa$$

The fourth Lamé-type task is related to the RVC loaded tangentially on boundary  $r = b$  in the longitudinal direction with the following shear stress:

$$\tau_{1rm}(b, \varphi) = \tau_0 \cos \varphi \quad (64)$$

This loading induces pure longitudinal shear. The general solutions have the following form (evidence included in [30]):

– stresses and displacements corresponding to the fibre ( $0 \leq r \leq a$ ):

$$\tau_{1rf}(\varphi) = G_{12f} A_f \cos \varphi, \quad u_{1f}(r, \varphi) = A_f r \cos \varphi \quad (65)$$

– stresses and displacements corresponding to the matrix ( $a \leq r \leq b$ ):

$$\tau_{1rm}(r, \varphi) = G_m(A - B/r^2) \cos \varphi, \quad u_{1m}(r, \varphi) = r(A + B/r^2) \cos \varphi \quad (66)$$

– stresses and displacements corresponding to the homogenized RVC ( $0 \leq r \leq b$ ):

$$\tau_{1r}(\varphi) = \tau_0 \cos \varphi, \quad u_1(r, \varphi) = \tau_0 r \cos \varphi / G_{12} \quad (67)$$

The stress boundary condition takes the form of Eqn. (64). The continuity conditions have the form

$$\tau_{1rf}(\varphi) = \tau_{1rm}(a, \varphi), \quad u_{1f}(a, \varphi) = u_{1m}(a, \varphi) \quad (68)$$

The compatibility condition has the form

$$u_{1m}(b, \varphi) = u_1(b, \varphi) \quad (69)$$

Equations (64), (68), (69) form a system of four linear algebraic equations with unknowns  $A_f, A, B, S_{s12h}$ . The solution to elastic compliance  $S_{s12h}$  has the form

$$S_{s12h} = s_s [2s_s(1 - f) G_{12f}/E_{1f} + 1 + f] / [2s_s(1 + f) G_{12f}/E_{1f} + 1 - f] / E_{1f} \quad (70)$$

The refined homogenization theory results in elastic compliances  $S_{11h}, S_{12h}, S_{22h}, S_{23h}, S_{s12h}$  defined respectively by Eqns. (48)<sub>1,2</sub>, (52)<sub>1</sub>, (61), (70). Compliances  $S_{22h}, S_{23h}$  are calculated from Eqns. (41). Taking into account Eqns. (39), the relationships

$$S_{11e} = S_{11h}, \quad S_{22e} = S_{22h}, \quad S_{12e} = S_{12h}, \quad S_{23e} = S_{23h}, \quad S_{s12e} = S_{s12h} \quad (71)$$

allow the EECs of a homogenized UFRP composite to be determined, i.e.

$$E_1 = 1/S_{11h}, \quad E_2 = 1/S_{22h}, \quad \nu_{12} = -E_1 S_{12h}, \quad \nu_{23} = -E_2 S_{23h}, \quad G_{12} = 1/2S_{s12h} \quad (72)$$

In order to validate experimentally the refined homogenization theory presented in this study, the predictions of EECs are computed for four UFRP composites analysed in [31, 32] and described previously in this Section, i.e. two composites reinforced with glass fibres (EGG/LHD, EGS/MHD) and two composites reinforced with carbon fibres (AS4/3501-6, T300/BSL). Table 2 summarizes the results of the experimental and simulation (prediction) studies on the EECs of the composites under consideration.

TABLE 2. EECs of UFRP composites under consideration – experiment and simulation

| EEC            | EGG/LHD |       | EGS/MHD |       | AS4/3501-6 |        | T300/BSL |        |
|----------------|---------|-------|---------|-------|------------|--------|----------|--------|
|                | Exp.    | Sim.  | Exp.    | Sim.  | Exp.       | Sim.   | Exp.     | Sim.   |
| $E_1$ [GPa]    | 53.48   | 50.90 | 45.6    | 45.76 | 126        | 136.70 | 138      | 139.63 |
| $E_2$ [GPa]    | 17.7    | 16.69 | 16.2    | 15.52 | 11         | 10.70  | 11       | 10.57  |
| $\nu_{12}$     | 0.278   | 0.249 | 0.278   | 0.252 | 0.28       | 0.253  | 0.28     | 0.257  |
| $\nu_{23}$     | 0.4     | 0.202 | 0.4     | 0.212 | 0.4        | 0.168  | 0.4      | 0.181  |
| $G_{12}$ [GPa] | 5.83    | 4.60  | 5.83    | 4.32  | 6.6        | 4.54   | 5.5      | 4.35   |

Note that as described in [31, 32], some of the experimental input or output data for carbon fibre-reinforced composites ( $E_{2f}, \nu_{12f}, \nu_{23f}, G_{12f}, \nu_{23}$ ) were estimated or adopted arbitrarily. The value of constant  $\nu_{23f} = 0.0714$  for both carbon-epoxy composites corresponds to an approximate value of  $G_{23f} = 7$  GPa.

Constant  $\nu_{23} = 0.4$  for glass-epoxy composites is of reduced reliability.

In light of Table 2 and the above remarks, the experimental validation of the refined homogenization theory can be evaluated positively. Due to the use of analytical solutions of the theory of linear elasticity, the EEC prediction results are of higher reliability, provided that the input data for the prediction is adequate and accurate.

## REFINED ELASTIC AND RHEOLOGICAL MODELLING OF UFRT COMPOSITES

The considerations in this section are an abbreviated version of those presented in [2], adopting a more natural system of designations. The  $x_1x_2x_3$  Cartesian coordinate system, common for an isotropic matrix and a monotropic UFRT composite, coincides with the principal directions of the homogenized composite, i.e.  $x_1$  – direction of fibres,  $x_2x_3$  – transverse isotropy plane. The stress and strain components in the composite are defined analogously to a thermoset (see Section 2).

The assumptions made in the rheological modelling of a UFRT composite are as follows:

- A UFRT composite is a new (unaged) material fully relaxed from the residual stresses induced by the manufacturing processes.
- A UFRT composite consists of two components, a thermoset matrix and fibres.
- The fibre is a linearly elastic monotropic material with the direction of monotropy coinciding with the fibre direction.
- The fibres have an identical circular cross-section.
- The fibres are perfectly bonded to the matrix; the interphase is neglected.
- The fibres are long, rectilinear, arranged unidirectionally and uniformly in the matrix in a hexagonal scheme.
- The thermoset matrix is a linearly viscoelastic isotropic material described by the H–R/H rheological model, as presented in Section 2.
- The homogenized UFRT composite is a monotropic material with the direction of monotropy coinciding with the fibre direction.
- The homogenized UFRT composite exhibits linearly viscoelastic shear strains and linearly elastic bulk strains.
- Quasi-static long-term isothermal rheological processes under normal conditions are considered.
- Appropriately low levels of stresses and strains secure the reversibility of the rheological processes.

The effective elastic shear and bulk modules of a UFRT composite, corresponding to the transverse isotropy plane, are defined as

$$\begin{aligned} G_{23} &= E_2/2(1 + \nu_{23}), \\ B_2 &= E_2/3(1 - 2\nu_{23}) \end{aligned} \quad (73)$$

Coupled standard constitutive equations of the linear elasticity of the homogenized UFRT composite (monotropic material) have the following form (based on [36])

$$\boldsymbol{\varepsilon} = \mathbf{S}_e \boldsymbol{\sigma}, \quad \boldsymbol{\delta} = \mathbf{S}_{se} \boldsymbol{\tau} \quad (74)$$

where:

$$\begin{aligned} \mathbf{S}_e &= \begin{bmatrix} S_{11e} & S_{12e} & S_{12e} \\ & S_{22e} & S_{23e} \\ \text{symm.} & & S_{22e} \end{bmatrix}, \\ \mathbf{S}_{se} &= \text{diag}(S_{s23e}, S_{s12e}, S_{s12e}) \end{aligned} \quad (75)$$

$$S_{11e} = 1/E_1, \quad S_{22e} = 1/E_2,$$

$$S_{12e} = -\nu_{12}/E_1, \quad S_{23e} = -\nu_{23}/E_2$$

$$S_{s23e} = 1/2G_{23}, \quad S_{s12e} = 1/2G_{12}$$

Vectors  $\boldsymbol{\varepsilon}, \boldsymbol{\delta}, \boldsymbol{\sigma}, \boldsymbol{\tau}$  are defined by Eqns. (3)<sub>1-4</sub>. Quantities  $\mathbf{S}_e, \mathbf{S}_{se}$  are elastic compliance matrices corresponding to normal/shear strains.

Coupled inverse constitutive equations of the linear elasticity of the homogenized UFRT composite have the following form (based on [36])

$$\boldsymbol{\sigma} = \mathbf{C}_e \boldsymbol{\varepsilon}, \quad \boldsymbol{\tau} = \mathbf{C}_{se} \boldsymbol{\delta} \quad (76)$$

where:

$$\begin{aligned} \mathbf{C}_e &= \mathbf{S}_e^{-1} = \begin{bmatrix} C_{11e} & C_{12e} & C_{12e} \\ & C_{22e} & C_{23e} \\ \text{symm.} & & C_{22e} \end{bmatrix}, \\ \mathbf{C}_{se} &= \mathbf{S}_{se}^{-1} = \text{diag}(C_{s23e}, C_{s12e}, C_{s12e}) \\ C_{11e} &= E_1(1 - \nu_{23}^2)/\Delta, \\ C_{22e} &= E_2(1 - \nu_{12}\nu_{21})/\Delta \\ C_{12e} &= E_2\nu_{12}(1 + \nu_{23})/\Delta, \\ C_{23e} &= E_2(\nu_{23} + \nu_{12}\nu_{21})/\Delta \\ C_{s23e} &= 2G_{23}, \quad C_{s12e} = 2G_{12} \\ \Delta &= 1 - \nu_{23}^2 - 2\nu_{12}\nu_{21}(1 + \nu_{23}) \end{aligned} \quad (77)$$

Quantities  $\mathbf{C}_e, \mathbf{C}_{se}$  are elastic stiffness matrices corresponding to normal/shear strains.

Uncoupled standard/inverse constitutive equations of the linear elasticity of the homogenized UFRT composite, equivalent respectively to Eqns. (74)<sub>1</sub> and (76)<sub>1</sub>, have the following form (evidence included in [2, 37])

$$\begin{aligned} \boldsymbol{\varepsilon}_s &= \mathbf{S}_{qse} \boldsymbol{\sigma}_s, \quad \boldsymbol{\varepsilon}_b = \mathbf{S}_{qbe} \boldsymbol{\sigma}_b \\ \boldsymbol{\sigma}_s &= \mathbf{C}_{qse} \boldsymbol{\varepsilon}_s, \quad \boldsymbol{\sigma}_b = \mathbf{C}_{qbe} \boldsymbol{\varepsilon}_b \end{aligned} \quad (78)$$

where:

$$\begin{aligned} \mathbf{S}_{qse} &= \text{diag}(S_{s1e}, S_{s23e}, S_{s23e}), \\ \mathbf{S}_{qbe} &= \text{diag}(S_{b1e}, S_{b2e}, S_{b2e}) \\ S_{s1e} &= (1 + \nu_{12}\lambda)/E_1, \\ S_{b1e} &= (1 - 2\nu_{12}\lambda)/E_1, \quad S_{b2e} = 1/3B_2 \\ \mathbf{C}_{qse} &= \mathbf{S}_{qse}^{-1} = \text{diag}(C_{s1e}, C_{s23e}, C_{s23e}), \\ \mathbf{C}_{qbe} &= \mathbf{S}_{qbe}^{-1} = \text{diag}(C_{b1e}, C_{b2e}, C_{b2e}) \\ C_{s1e} &= E_1/(1 + \nu_{12}\lambda), \quad C_{b1e} = E_1/(1 - 2\nu_{12}\lambda), \\ & \quad C_{b2e} = 3B_2 \end{aligned} \quad (79)$$

and

$$\begin{aligned} \boldsymbol{\varepsilon}_s &= (\mathbf{I} - \mathbf{B})\boldsymbol{\varepsilon}, \quad \boldsymbol{\sigma}_s = (\mathbf{I} - \mathbf{A})\boldsymbol{\sigma}, \quad \boldsymbol{\varepsilon}_b = \mathbf{B}\boldsymbol{\varepsilon}, \quad \boldsymbol{\sigma}_b = \mathbf{A}\boldsymbol{\sigma} \\ \mathbf{I} &= \text{diag}(1, 1, 1), \quad \mathbf{A} = \frac{1}{3} \begin{bmatrix} 1 & 1/\lambda & 1/\lambda \\ \lambda & 1 & 1 \\ \lambda & 1 & 1 \end{bmatrix}, \quad \mathbf{B} = \mathbf{D}(\mathbf{C}_e - \mathbf{C}_{qse}) \\ \lambda &= \nu_{21}/\nu_{23}, \quad \nu_{21} = \nu_{12} E_2/E_1 \\ \mathbf{D} &= \text{diag}(D_1, D_2, D_2), \quad D_1 = 1/(C_{b1e} - C_{s1e}), \\ & \quad D_2 = 1/(C_{b2e} - C_{s23e}) \end{aligned} \tag{80}$$

The following nomenclature and interpretation are introduced:  $\boldsymbol{\varepsilon}_s, \boldsymbol{\varepsilon}_b, \boldsymbol{\sigma}_s, \boldsymbol{\sigma}_b$  – vectors of the elastic quasi-shear/quasi-bulk strains/stresses in a monotropic material,  $\mathbf{S}_{qse}, \mathbf{S}_{qbe}$  – elastic quasi-shear/quasi-bulk compliance matrices describing a monotropic material,  $\mathbf{C}_{qse}, \mathbf{C}_{qbe}$  – elastic quasi-shear/quasi-bulk stiffness matrices describing a monotropic material,  $\mathbf{I}, \mathbf{A}, \mathbf{B}$  – transformation matrices,  $\lambda$  – monotropy ratio. Note that  $\boldsymbol{\varepsilon} = \boldsymbol{\varepsilon}_s + \boldsymbol{\varepsilon}_b, \boldsymbol{\sigma} = \boldsymbol{\sigma}_s + \boldsymbol{\sigma}_b$ . In addition, it can be demonstrated that (evidence included in [2])

$$\begin{aligned} \mathbf{S}_e &= \mathbf{S}_{qse}(\mathbf{I} - \mathbf{A}) + \mathbf{S}_{qbe}\mathbf{A}, \\ \mathbf{C}_e &= \mathbf{C}_{qse}(\mathbf{I} - \mathbf{B}) + \mathbf{C}_{qbe}\mathbf{B} \end{aligned} \tag{81}$$

The shear-bulk decoupling of Eqns. (74)<sub>1</sub> and (76)<sub>1</sub> allows the results of the rheological modelling of the thermoset (presented in Section 2) to be generalized to model the homogenized UFRT composite.

Uncoupled standard constitutive equations of the linear rheology of the homogenized UFRT composite, corresponding to Eqns. (78)<sub>1,2</sub>, (74)<sub>2</sub>, are predicted in the following form (compare with Eqns. (10)):

$$\begin{aligned} \boldsymbol{\varepsilon}_s(t) &= \mathbf{S}_{qs}(t) \otimes \boldsymbol{\sigma}_s(t), \\ \boldsymbol{\varepsilon}_b(t) &= \mathbf{S}_{qbe}\boldsymbol{\sigma}_b(t), \quad \boldsymbol{\delta}(t) = \mathbf{S}_s(t) \otimes \boldsymbol{\tau}(t) \end{aligned} \tag{82}$$

for time variable  $t \geq 0$ , with

$$\begin{aligned} \mathbf{S}_{qs}(t) &= \text{diag}[S_{s1}(t), S_{s23}(t), S_{s23}(t)] \\ \mathbf{S}_s(t) &= \text{diag}[S_{s23}(t), S_{s12}(t), S_{s12}(t)] \\ S_{s1}(t) &= S_{s1e} \left[ 1 + c_1 \int_0^t \Phi(v) dv \right] \\ S_{sjk}(t) &= S_{sjke} \left[ 1 + c_{jk} \int_0^t \Phi(v) dv \right], \quad jk = 23, 12 \tag{83} \\ \Phi(t) &= \frac{1}{T_c} \int_0^\infty \exp\left(-\frac{ut}{T_c}\right) u L(u) du \\ L(u) &= \frac{\sin \pi r}{\pi u} \frac{u^r}{1 + 2u^r \cos \pi r + u^{2r}}, \quad 0 < r < 1 \end{aligned}$$

The nomenclature and interpretation are as follows:  $L(u)$  – function defining a Mittag-Leffler fractional exponential function in an integral form,  $r$  – fraction defining a Mittag-Leffler fractional exponential function in an integral form,  $T_c$  – retardation time,  $\Phi(t)$  – a Mittag-Leffler fractional exponential generic function in an integral form for shear/quasi-shear stresses,  $\mathbf{S}_{qs}(t)$  – elastic-viscoelastic quasi-shear compliance matrix,

$\mathbf{S}_s(t)$  – elastic-viscoelastic shear compliance matrix,  $c_1, c_{23}, c_{12}$  – long-term creep coefficients,  $\otimes$  – convolution product operator.

A linear rheological model of the homogenized UFRT composite, governed by Eqns. (82), (83), is also denoted H-R/H. Under the assumptions made, the composite is described by five independent elastic constants ( $E_1, E_2, \nu_{12}, \nu_{23}, G_{12}$ ) and five independent viscoelastic constants ( $T_c, r, c_1, c_{23}, c_{12}$ ). A mechanical representation of the H-R/H model for the homogenized UFRT composite consists of three uncoupled H-R subsystems and two uncoupled H subsystems.

Constants  $T_c, r$  are determined experimentally for the thermoset matrix and are common to the matrix and the UFRT composite. This hypothesis will be confirmed in further considerations for the selected UFRT composites. An analytical algorithm for determining constants  $c_1, c_{23}, c_{12}$ , based on the homogenization theory for a UFRT composite with monotropic fibres and VECP, will be formulated in further considerations.

The general formulation of a creep stress programme is

$$\boldsymbol{\sigma}_s(t) = \boldsymbol{\sigma}_{s0}H(t), \quad \boldsymbol{\sigma}_b(t) = \boldsymbol{\sigma}_{b0}H(t), \quad \boldsymbol{\tau}(t) = \boldsymbol{\tau}_0H(t) \tag{84}$$

where:  $\boldsymbol{\sigma}_{s0}, \boldsymbol{\sigma}_{b0}, \boldsymbol{\tau}_0$  – quasi-shear, quasi-bulk, and shear constant stresses in a differential volume of the composite. The strain response to the creep stress programme has the form

$$\begin{aligned} \boldsymbol{\varepsilon}_s(t) &= \mathbf{S}_{qsc}(t)\boldsymbol{\sigma}_{s0}, \quad \boldsymbol{\varepsilon}_b(t) = \mathbf{S}_{qbe}\boldsymbol{\sigma}_{b0}, \\ \boldsymbol{\delta}(t) &= \mathbf{S}_{sc}(t)\boldsymbol{\tau}_0 \end{aligned} \tag{85}$$

where:

$$\begin{aligned} \mathbf{S}_{qsc}(t) &= \text{diag}[S_{s1c}(t), S_{s23c}(t), S_{s23c}(t)] \\ \mathbf{S}_{sc}(t) &= \text{diag}[S_{s23c}(t), S_{s12c}(t), S_{s12c}(t)] \\ S_{s1c}(t) &= S_{s1e}[1 + c_1\varphi(t)], \\ S_{sjkc}(t) &= S_{sjke}[1 + c_{jk}\varphi(t)], \quad jk = 23, 12 \end{aligned} \tag{86}$$

Creep function  $\varphi(t)$  is defined by Eqn. (14).

Complex compliances of the homogenized UFRT composite are expressed as:

$$\begin{aligned} S_{s1}^*(\omega) &= S_{s1}'(\omega) + iS_{s1}''(\omega) \\ S_{sjk}^*(\omega) &= S_{sjk}'(\omega) + iS_{sjk}''(\omega) \\ S_{s1}'(\omega) &= S_{s1e}[1 + c_1M(\omega T_c, r)] \\ S_{s1}''(\omega) &= -S_{s1e}c_1N(\omega T_c, r) \\ S_{sjk}'(\omega) &= S_{sjke}[1 + c_{jk}M(\omega T_c, r)] \\ S_{sjk}''(\omega) &= -S_{sjke}c_{jk}N(\omega T_c, r), \quad jk = 23, 12 \\ M(\omega T_c, r) &= \frac{1 + (\omega T_c)^r \cos(\pi r/2)}{1 + 2(\omega T_c)^r \cos(\pi r/2) + (\omega T_c)^{2r}} \\ N(\omega T_c, r) &= \frac{(\omega T_c)^r \sin(\pi r/2)}{1 + 2(\omega T_c)^r \cos(\pi r/2) + (\omega T_c)^{2r}} \end{aligned} \tag{87}$$

with the following interpretation and nomenclature:  $S_{s1}^*(\omega), S_{sjk}^*(\omega)$  – complex quasi-shear/shear compliances,  $S_{s1}'(\omega), S_{sjk}'(\omega)$  – quasi-shear/shear storage compliances,  $S_{s1}''(\omega), S_{sjk}''(\omega)$  – quasi-shear/shear loss

compliances. The storage and loss compliances have properties analogous to those described by Eqns. (A.3) in Appendix A.

Uncoupled inverse constitutive equations of the linear rheology of the homogenized UFRT composite have the following form:

$$\begin{aligned} \boldsymbol{\sigma}_s(t) &= \mathbf{C}_{qs}(t) \otimes \boldsymbol{\varepsilon}_s(t) \\ \boldsymbol{\sigma}_b(t) &= \mathbf{C}_{qbe} \boldsymbol{\varepsilon}_b(t), \quad \boldsymbol{\tau}(t) = \mathbf{C}_s(t) \otimes \boldsymbol{\delta}(t) \end{aligned} \quad (88)$$

for time variable  $t \geq 0$ , with:

$$\begin{aligned} \mathbf{C}_{qs}(t) &= \text{diag} [C_{s1}(t), C_{s23}(t), C_{s23}(t)], \\ \mathbf{C}_s(t) &= \text{diag} [C_{s23}(t), C_{s12}(t), C_{s12}(t)] \\ C_{s1}(t) &= C_{s1e} \left[ 1 - d_1 \int_0^t \Psi_1(v) dv \right] \\ \Psi_1(t) &= \frac{1}{T_{d1}} \int_0^\infty \exp\left(-\frac{ut}{T_{d1}}\right) u L(u) du \\ C_{sjk}(t) &= C_{sjke} \left[ 1 - d_{jk} \int_0^t \Psi_{jk}(v) dv \right] \\ \Psi_{jk}(t) &= \frac{1}{T_{djk}} \int_0^\infty \exp\left(-\frac{ut}{T_{djk}}\right) u L(u) du \\ d_1 &= \frac{c_1}{1 + c_1}, \quad T_{d1} = T_c \exp\left(\frac{1}{r} \ln \frac{1}{1 + c_1}\right) \\ d_{jk} &= \frac{c_{jk}}{1 + c_{jk}}, \quad T_{djk} = T_c \exp\left(\frac{1}{r} \ln \frac{1}{1 + c_{jk}}\right), \quad jk = 23, 12 \end{aligned} \quad (89)$$

The following nomenclature and interpretation are introduced:  $T_{d1}, T_{djk}$  – relaxation times,  $\Psi_1(t), \Psi_{jk}(t)$  – strain generic functions,  $\mathbf{C}_{qs}(t)$  – elastic-viscoelastic quasi-shear stiffness matrix,  $\mathbf{C}_s(t)$  – elastic-viscoelastic shear stiffness matrix,  $d_1, d_{jk}$  – long-term relaxation coefficients. Viscoelastic parameters  $d_1, d_{jk}, T_{d1}, T_{djk}$  are expressed in terms of previous viscoelastic parameters  $c_1, c_{jk}, T_c$ , as specified in Eqns. (89)<sub>7-10</sub>. Function  $L(u)$  is defined by Eqn. (83)<sub>6</sub> equivalent to Eqn. (11)<sub>3</sub>.

The general formulation of a relaxation strain programme is

$$\begin{aligned} \boldsymbol{\varepsilon}_s(t) &= \boldsymbol{\varepsilon}_{s0} H(t), \quad \boldsymbol{\varepsilon}_b(t) = \boldsymbol{\varepsilon}_{b0} H(t), \\ \boldsymbol{\delta}(t) &= \boldsymbol{\delta}_0 H(t) \end{aligned} \quad (90)$$

where:  $\boldsymbol{\varepsilon}_{s0}, \boldsymbol{\varepsilon}_{b0}, \boldsymbol{\delta}_0$  – quasi-shear, quasi-bulk, and shear constant strains in a differential volume of the composite. The stress response to the relaxation strain programme has the form:

$$\begin{aligned} \boldsymbol{\sigma}_s(t) &= \mathbf{C}_{qsr}(t) \boldsymbol{\varepsilon}_{s0}, \quad \boldsymbol{\sigma}_b(t) = \mathbf{C}_{qbe} \boldsymbol{\varepsilon}_{b0}, \\ \boldsymbol{\tau}(t) &= \mathbf{C}_{sr}(t) \boldsymbol{\delta}_0 \end{aligned} \quad (91)$$

where:

$$\begin{aligned} \mathbf{C}_{qsr}(t) &= \text{diag} [C_{s1r}(t), C_{s23r}(t), C_{s23r}(t)] \\ \mathbf{C}_{sr}(t) &= \text{diag} [C_{s23r}(t), C_{s12r}(t), C_{s12r}(t)] \\ C_{s1r}(t) &= C_{s1e} [1 - d_1 \psi_1(t)], \\ C_{sjkr}(t) &= C_{sjke} [1 - d_{jk} \psi_{jk}(t)], \quad jk = 23, 12 \end{aligned} \quad (92)$$

with relaxation functions:

$$\begin{aligned} \psi_1(t) &= \int_0^t \Psi_1(v) dv = 1 - \int_0^\infty \exp\left(-\frac{ut}{T_{d1}}\right) L(u) du \\ \psi_{jk}(t) &= \int_0^t \Psi_{jk}(v) dv = 1 - \int_0^\infty \exp\left(-\frac{ut}{T_{djk}}\right) L(u) du, \\ jk &= 23, 12 \end{aligned} \quad (93)$$

Coupled standard/inverse constitutive equations of the linear rheology of the homogenized UFRT composite result from Eqns. (80)<sub>1-4</sub>, (82), (88), i.e.:

$$\begin{aligned} \boldsymbol{\varepsilon}(t) &= \mathbf{S}(t) \otimes \boldsymbol{\sigma}(t), \quad \boldsymbol{\delta}(t) = \mathbf{S}_s(t) \otimes \boldsymbol{\tau}(t) \\ \boldsymbol{\sigma}(t) &= \mathbf{C}(t) \otimes \boldsymbol{\varepsilon}(t), \quad \boldsymbol{\tau}(t) = \mathbf{C}_s(t) \otimes \boldsymbol{\delta}(t) \end{aligned} \quad (94)$$

where:

$$\begin{aligned} \mathbf{S}(t) &= \mathbf{S}_{qs}(t) (\mathbf{I} - \mathbf{A}) + \mathbf{S}_{qbe} \mathbf{A}, \\ \mathbf{C}(t) &= \mathbf{C}_{qs}(t) (\mathbf{I} - \mathbf{B}) + \mathbf{C}_{qbe} \mathbf{B} \end{aligned} \quad (95)$$

are the elastic-viscoelastic compliance and stiffness matrices of a homogeneous monotropic material. Transformation matrices  $\mathbf{I}, \mathbf{A}, \mathbf{B}$  are defined by Eqns. (80)<sub>5-11</sub>.

Equations (94) can be rewritten in the following equivalent form:

$$\begin{aligned} \boldsymbol{\varepsilon}(t) &= \mathbf{S}_e \boldsymbol{\sigma}(t) + \mathbf{S}_v(t) (\mathbf{I} - \mathbf{A}) \otimes \boldsymbol{\sigma}(t), \\ \boldsymbol{\delta}(t) &= \mathbf{S}_{se} \boldsymbol{\tau}(t) + \mathbf{S}_{sv}(t) \otimes \boldsymbol{\tau}(t) \\ \boldsymbol{\sigma}(t) &= \mathbf{C}_e \boldsymbol{\varepsilon}(t) + \mathbf{C}_v(t) (\mathbf{I} - \mathbf{B}) \otimes \boldsymbol{\varepsilon}(t), \\ \boldsymbol{\tau}(t) &= \mathbf{C}_{se} \boldsymbol{\delta}(t) + \mathbf{C}_{sv}(t) \otimes \boldsymbol{\delta}(t) \end{aligned} \quad (96)$$

where:

$$\begin{aligned} \mathbf{S}_v(t) &= \text{diag} [S_{v1}(t), S_{v23}(t), S_{v23}(t)] \\ \mathbf{S}_{sv}(t) &= \text{diag} [S_{v23}(t), S_{v12}(t), S_{v12}(t)] \\ S_{v1}(t) &= S_{s1e} c_1 \int_0^t \Phi(v) dv \\ S_{vjk}(t) &= S_{sjke} c_{jk} \int_0^t \Phi(v) dv, \quad jk = 23, 12 \\ \mathbf{C}_v(t) &= \text{diag} [C_{v1}(t), C_{v23}(t), C_{v23}(t)] \\ \mathbf{C}_{sv}(t) &= \text{diag} [C_{v23}(t), C_{v12}(t), C_{v12}(t)] \\ C_{v1}(t) &= -C_{s1e} d_1 \int_0^t \Psi_1(v) dv, \\ C_{vjk}(t) &= -C_{sjke} d_{jk} \int_0^t \Psi_{jk}(v) dv, \quad jk = 23, 12 \end{aligned} \quad (97)$$

Generic functions:  $\Phi(t), \Psi_1(t), \Psi_{jk}(k), jk = 23, 12$  are defined by Eqns. (83)<sub>5,6</sub>, (89)<sub>4,6</sub>. Equations (96) highlight the separation of the elastic parts from the viscoelastic parts of the UFRT composite response.

## REFINED FORMULATION OF COMPLEMENTARY PROBLEMS PRESENTED IN [29]

Function  $L(u), 0 < r < 1$ , defining a Mittag-Leffler fractional exponential function in an integral form (Eqn. (11)<sub>3</sub>), is an intermediate continuous function between Dirac function  $\delta(u = 1)$  for  $r = 1$  and Dirac

function  $\delta(u = 0)$  for  $r = 0$ , and contains a singularity at point  $u = 0$  (Eqns. (A.1)<sub>1-3</sub> in Appendix A). A general integral

$$J = \int_0^\infty f(u) du \quad (98)$$

with subintegral function  $f(u)$  containing  $L(u)$  is calculated numerically using a high-rank  $n$ -point Gauss-Legendre quadrature (evidence included in [29])

$$J \approx 2 \sum_{k=1}^n [w_k f(u_k) / (1 + x_k)^2] \\ u_k = (1 - x_k) / (1 + x_k) \quad (99)$$

Quantities  $w_k, x_k, k = 1, 2, \dots, n$ , are the weights and nodes of the  $n$ -point quadrature. Each subintegral function is approximated with a  $(2n + 1)$ th degree polynomial. Equations (99) are used for integrals occurring in functions  $T_c \Phi(\tau), \varphi(\tau)$ , whereby  $\tau = t/T_c, u^r = \exp(r \ln u)$ . The most accurate quadrature of degree available  $n = 32$  [38] was used (evidence included in [29]).

To identify the isotropic thermoset matrix material constants describing the H-R/H rheological model, a stress-controlled tension creep test was used, performed experimentally on the thermoset sample in direction  $x_1$ . The creep process is preceded by a relatively rapid linear increase in stress  $\sigma_1(t)$  to the level  $\sigma_{10} > 0$ , which induces a quasi-linear increase in longitudinal strain  $\varepsilon_1(t)$  to the level  $\varepsilon_{10} > 0$ , as well as to a quasi-linear decrease in transverse strain  $\varepsilon_2(t)$  to the level  $\varepsilon_{20} < 0$ . Note that  $\varepsilon_3(t) = \varepsilon_2(t)$ . The elastic constants of the thermoset are identified from the classical equations

$$E_m = \Delta\sigma_1 / \Delta\varepsilon_1, \quad \nu_m = -\Delta\varepsilon_2 / \Delta\varepsilon_1 \quad (100)$$

where  $\Delta\sigma_1, \Delta\varepsilon_1, \Delta\varepsilon_2$  are stress/strain increments that precede the extreme values  $\sigma_{10}, \varepsilon_{10}, \varepsilon_{20}$ , respectively. Stress level  $\sigma_{10}$  was assumed to provide the reversibility of creep strains.

After reaching stress level  $\sigma_{10}$ , the sample is subjected to creep under stress  $\sigma_{10}$  over time interval  $t \in [0, T_1]$ , where  $T_1$  – long-term creep time. The recorded experimental directional strains  $\varepsilon_{1E}(t), \varepsilon_{2E}(t)$  are converted to experimental shear and bulk strains (see Eqns. (6) and (7))

$$\varepsilon_{s1E}(t) = \frac{2}{3} [\varepsilon_{1E}(t) - \varepsilon_{2E}(t)], \\ \varepsilon_{bE}(t) = \frac{1}{3} [\varepsilon_{1E}(t) + 2\varepsilon_{2E}(t)] \quad (101)$$

induced by

$$\sigma_{s1E} = \frac{2}{3} \sigma_{10}, \quad \sigma_{bE} = \frac{1}{3} \sigma_{10} \quad (102)$$

The H-R/H rheological model results in approximate equations (see Eqns. (6)<sub>1</sub>, (13)<sub>1</sub>)

$$\varepsilon_{s1E}(t) = [1 + c\varphi(\tau)]\varepsilon_{s1E}(0), \\ \varepsilon_{bE}(t) = \varepsilon_{bE}(0), \quad t \geq 0 \quad (103)$$

with  $\tau = t/T_c$ . The values of the simulation creep function  $\varphi(\tau)$  corresponding to the creep times ( $T_c, 0.1T_c$ ) are denoted as

$$a = \varphi(1), \quad b = \varphi(0.1) \quad (104)$$

The readings from experimental graph  $\varepsilon_{s1E}(t)$  and the final calculation accuracy are recommended to 3 meaningful digits.

An analytical iterative algorithm to identify viscoelastic constants  $T_c, c, r$ , based on Eqn. (103)<sub>1</sub> is presented in [29]. An abbreviated refined description of this algorithm is provided below. Abscissa  $y = \log t$  corresponding to the inflection point on chart  $\varepsilon_{s1E}(t)$  on a logarithmic time scale is read, hence  $T_c = \exp(y \ln 10)$ . The value of fraction  $r$  is predicted and  $a(r)$  is calculated. The other constants are calculated from the following equations:

$$c = [\varepsilon_{s1E}(T_c) / \varepsilon_{s1E}(0) - 1] / a, \\ b = [\varepsilon_{s1E}(0.1T_c) / \varepsilon_{s1E}(0) - 1] / c \quad (105)$$

The next iteration, if any, is preceded by the calculation of  $r(b)$  and  $a(b)$ .

Once constants  $T_c, r, c$  are determined, the simulation shear strain graph is calculated, i.e.

$$\varepsilon_{s1}(t) = [1 + c\varphi(\tau)]\varepsilon_{s1E}(0), \quad t \in [0, T_1] \quad (106)$$

and presented on a logarithmic time scale ( $y = \log t$ ) against the experimental shear strain graph. A set of  $m$  quasi-equally spaced collocation points on a logarithmic time scale are chosen. The relative error is

$$\delta = \sum_{j=1}^m |\varepsilon_{s1}(t_j) - \varepsilon_{s1E}(t_j)| / \sum_{j=1}^m \varepsilon_{s1E}(t_j) \quad (107)$$

whereby:

$$\varepsilon_{s1}(t_j) = [1 + c\varphi(\tau_j)]\varepsilon_{s1E}(0) \\ \tau_j = t_j / T_c, \quad \varphi(\tau_j) = 1 - \int_0^\infty \exp(-u\tau_j) L(u) du, \quad (108) \\ t_j = 10^{y_j}, \quad j = 1, 2, \dots, m$$

Constant  $r$  appears in function  $L(u)$ .

According to the H-R/H rheological model formulated in Section 4, the homogenized UFRT composite is described by five viscoelastic constants  $T_c, r, c_1, c_{23}, c_{12}$ . Constants  $T_c, r$  are common to the matrix and the composite. Long-term creep coefficients  $c_1, c_{23}, c_{12}$  can be determined analytically using VECP (the viscoelastic-elastic correspondence principle).

Unconjugated standard constitutive equations of the linear elasticity of the homogenized UFRT composite (78)<sub>1,2</sub>, (74)<sub>2</sub> are expressed in terms of quasi-shear/shear elastic compliances  $S_{s1e}, S_{s23e}, S_{s12e}$ . Based on Eqns. (71), (75)<sub>3,5</sub>, (79)<sub>3</sub>, one obtains

$$S_{s1h} = S_{s11h} - \lambda S_{s12h} \quad (109)$$

As a result of the improved homogenization theory developed in this study, elastic compliances

$S_{s1h}(s_s, s_b)$ ,  $S_{s_jkh}(s_s, s_b)$ ,  $jk = 23, 12$ , are dependent on dimensionless elastic compliances of the thermoset matrix.

The complex compliances of the homogenized UFRT composite defined by Eqns. (87) can be rewritten in the following dimensionless form:

$$\begin{aligned} s_{s1}^*(\alpha) &= S_{s1}^*(\alpha)/S_{s1e} = s_{s1}'(\alpha) + is_{s1}''(\alpha) \\ s_{s1}'(\alpha) &= 1 + c_1 M(\alpha), \quad s_{s1}''(\alpha) = -c_1 N(\alpha) \\ s_{s_jk}^*(\alpha) &= S_{s_jk}^*(\alpha)/S_{s_jke} = s_{s_jk}'(\alpha) + is_{s_jk}''(\alpha) \\ s_{s_jk}'(\alpha) &= 1 + c_{jk} M(\alpha), \\ s_{s_jk}''(\alpha) &= -c_{jk} N(\alpha), \quad jk = 23, 12 \quad (110) \\ M(\alpha) &= \frac{1 + \alpha^r \cos(\pi r/2)}{1 + 2\alpha^r \cos(\pi r/2) + \alpha^{2r}}, \\ N(\alpha) &= \frac{\alpha^r \sin(\pi r/2)}{1 + 2\alpha^r \cos(\pi r/2) + \alpha^{2r}}, \quad \alpha = \omega T_c \end{aligned}$$

Quantities  $s_{s1}'(\alpha)$ ,  $s_{s_jk}'(\alpha)$ ,  $jk = 23, 12$ , were called H-R/H storage compliances.

The complex compliances of a homogenized UFRT composite calculated using VECP are expressed by the following formulas:

$$\begin{aligned} s_{s1h}^*(\alpha) &= S_{s1h}[s_s^*(\alpha), s_b]/S_{s1e} = \\ &= s_{s1h}'(\alpha) + is_{s1h}''(\alpha) \quad (111) \\ s_{s_jkh}^*(\alpha) &= S_{s_jkh}[s_s^*(\alpha), s_b]/S_{s_jke} = \\ &= s_{s_jkh}'(\alpha) + is_{s_jkh}''(\alpha), \quad jk = 23, 12 \end{aligned}$$

where, based on Eqns. (20), (37)<sub>3</sub>, (54)<sub>7-9</sub>,

$$\begin{aligned} s_s^*(\alpha) &= s_s'(\alpha) + is_s''(\alpha) \\ s_s'(\alpha) &= s_s[1 + cM(\alpha)] \quad (112) \\ s_s''(\alpha) &= -s_s cN(\alpha) \end{aligned}$$

are respectively the dimensionless complex shear compliance, shear storage compliance, and shear loss compliance of the thermoset matrix. Quantities  $s_{s1h}'(\alpha)$ ,  $s_{s_jkh}'(\alpha)$ ,  $jk = 23, 12$ , were called VECP storage compliances.

Viscoelastic constants  $c_1, c_{23}, c_{12}$  are determined from the following conditions (evidence included in [29]):

$$\begin{aligned} s_{s1}'(\alpha_d) &= s_{s1h}'(\alpha_d) \\ s_{s_jk}'(\alpha_d) &= s_{s_jkh}'(\alpha_d), \quad jk = 23, 12 \quad (113) \end{aligned}$$

where  $\alpha_d = 0.159$  is the value at which conditions  $M(\alpha) \approx 0.5$ ,  $N(\alpha) = \min$  are met. Inserting Eqns. (110)<sub>2,5</sub> into Eqns. (113) yields

$$\begin{aligned} c_1 &= [s_{s1h}'(\alpha_d) - 1]/M(\alpha_d) \\ c_{jk} &= [s_{s_jkh}'(\alpha_d) - 1]/M(\alpha_d), \quad jk = 23, 1 \quad (114) \end{aligned}$$

To validate the H-R/H rheological model of the homogenized UFRT composite, the relative errors of deviation of graphs  $s_{s1}'(\alpha), s_{s_jk}'(\alpha), jk = 23, 12$  from respective graphs  $s_{s1h}'(\alpha), s_{s_jkh}'(\alpha), jk = 23, 12$  are used, defined as

$$\begin{aligned} \delta_1 &= \sum_{i=1}^P |s_{s1}'(\alpha_i) - s_{s1h}'(\alpha_i)| / \sum_{i=1}^P s_{s1h}'(\alpha_i) \\ \delta_{jk} &= \sum_{i=1}^P |s_{s_jk}'(\alpha_i) - s_{s_jkh}'(\alpha_i)| / \sum_{i=1}^P s_{s_jkh}'(\alpha_i), \quad (115) \\ & \quad jk = 23, 12 \end{aligned}$$

whereby  $\alpha_i = 2\pi x_i$ ,  $x_i = i \cdot \Delta x$ ,  $i = 1, 2, \dots, P$ .

## NUMERICAL ANALYSES

The computations were performed using the authors' own computer programme written in Pascal. The computational paths are as follows:

- 1) testing the accuracy of the integration of improper integrals containing a Mittag-Leffler fractional exponential generic function, by means of high-rank Gauss-Legendre quadratures,
- 2) numerical analysis of creep functions defined by a Mittag-Leffler fractional exponential generic function,
- 3) numerical analysis of the complex compliance of a thermoset, corresponding to a Mittag-Leffler fractional exponential generic function,
- 4) identification of the viscoelastic constants of a thermoset corresponding to the H-R/H rheological model, based on the unidirectional tension creep experimental test data,
- 5) calculation of the EECs of a UFRT composite, based on the refined homogenization theory,
- 6) numerical analysis of the complex compliances of a UFRT composite, corresponding to a Mittag-Leffler fractional exponential generic function,
- 7) identification of the effective viscoelastic constants of a UFRT composite corresponding to the H-R/H rheological model using VECP.

The results of testing the accuracy of the integration of improper integrals are presented in [29]. Quadratures of degrees  $n = 15, 25, 32$  were tested with the nodes and weights taken from [38]. The most accurate quadrature of degree available,  $n = 32$ , was applied in the subsequent paths. The graphs of creep function  $\varphi(\tau)$  were shown on a semi-logarithmic scale with abscissa  $x = \log \tau$  and analysed in [29]. The values of the creep function at points  $T_c, 0.1T_c$ , corresponding to the selected values of ratio  $r$ , i.e.  $a = \varphi(1)$ ,  $b = \varphi(0.1)$ , are given in [29].

Numerical validation of the H-R/H rheological model of UFRT composites was carried out on the selected enhanced reliability UFRT composites considered in [31, 32], i.e. EGS/MHD (glass/epoxy), T300/BSL (carbon/epoxy). The elastic constants of the constituents as well as fibre volume fractions provided in [31] are cited in this study. The simulated EECs of these composites, based on the improved homogenization theory, are listed in Table 2.

Due to the lack of publications on experimental creep tests on MHD and BSL epoxy resins, the unidirectional tension creep experimental test on Epidian 53

epoxy resin presented in [24] was used to simulate the shear/quasi-shear storage compliances of the composites under study. The test was performed on a new sample made of Epidian 53 structural epoxy resin (former manufacturer Organika Sarzyna Chemical Plants, Sarzyna, Poland) under near-normal conditions. The experiment was conducted in 2002 at the Laboratory of Strength of Materials and Structures, Faculty of Mechanical Engineering, Military University of Technology, Warsaw, Poland (<https://imiio.wim.wat.edu.pl>), using a lever creeper without a thermal chamber.

According to the Technical Data Sheet of Epidian 53 resin, the basic material constants are: tensile strength  $R_t = 52$  MPa, ultimate longitudinal strain  $\epsilon_t = 2.4\% = 0.0240 = 24000 \mu\epsilon$ , heat distortion temperature  $T_h = 55$  °C, where  $\mu\epsilon$  denotes micro strain ( $1 \mu\epsilon = 10^{-6}$ ).

The unidirectional tension creep experimental test was performed according to the experiment conditions described in this study. The longitudinal normal stress was  $\sigma_{10} = 0.30R_t = 15.6$  MPa, which guaranteed reversibility of the creep process. From the pre-creep stress rapid increase process, the following parameters were identified:

$$\begin{aligned} E_m &= 3.14 \text{ GPa}, \nu_m = 0.418 \\ \epsilon_{10} &= 4970 \mu\epsilon, \epsilon_{20} = -2080 \mu\epsilon \\ \epsilon_{s1E}(0) &= 4700 \mu\epsilon, \epsilon_{bE}(0) = 270 \mu\epsilon \end{aligned}$$

Figure 1 presents the original graphs of experimental directional strains  $\epsilon_{1E}(t), \epsilon_{2E}(t)$ , recorded in interval  $[0, T_1]$ ,  $T_1 = 10^5$  min. A progressive recording time step from 0.005 min to 275 min was applied. According to the prediction of reversible creep, the strain rates decrease monotonically.

Figure 2 shows experimental directional strains  $\epsilon_{1E}(t), \epsilon_{2E}(t)$  on a logarithmic time scale. The levels of the elastic strains are indicated by dashed lines. The charts were used to identify the viscoelastic constants. Note that the long-term creep time  $T_1 = 10^5$  min (~70 days) would have to be extended by at least 10 times to completely prove the creep reversibility hypothesis. Moreover, an experimental recovery test after removing the unidirectional tension stress would be required. The interpretation of small oscillations in the strain patterns on a logarithmic time scale requires additional creep tests performed on a set of samples using a thermal chamber.

Figure 3 shows the shear and bulk strains on a logarithmic time scale, corresponding to the epoxy creep test, calculated according to Eqns. (101). The levels of elastic strains are marked with dashed lines. The constant bulk strain hypothesis was fully confirmed.

The results of the identifying the viscoelastic constants of the Epidian 53 epoxy resin are as follows:  $T_c = 70800$  min,  $c = 1.40$ ,  $r = 0.540$ . The relative error of the deviation of the  $\epsilon_{s1}(t)$  simulation graph from the  $\epsilon_{s1E}(t)$  experimental graph on a logarithmic time scale, calculated in interval  $x = \log t \in [-1, 5]$  ( $t \in [0.1 \text{ min}, 10^5 \text{ min}]$ ) is  $\delta = 2.3\%$  (Fig. 4).

The H-R/H model was assessed as adequate ( $10^5$  min  $\approx 70$  days). The long-term shear strain value predicted by Eqn. (106) is  $\epsilon_{s1}(\infty) = (1 + c)\epsilon_{s1E}(0) = 11280 \mu\epsilon$ . The long-term relaxation coefficient and relaxation time of the Epidian 53 epoxy resin calculated from Eqns. (22)<sub>1</sub>, (23) are  $d = 0.583$ ,  $T_d = 14000$  min.

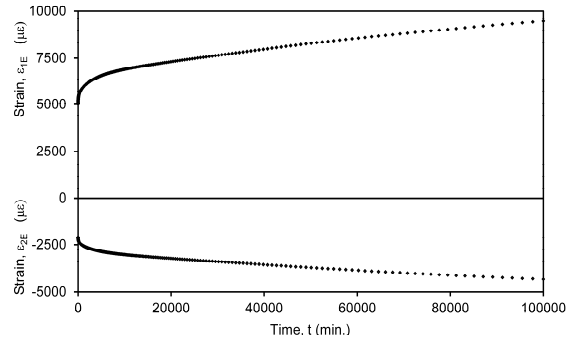


Fig. 1. Directional strains in unidirectional tension creep experimental test on epoxy specimen

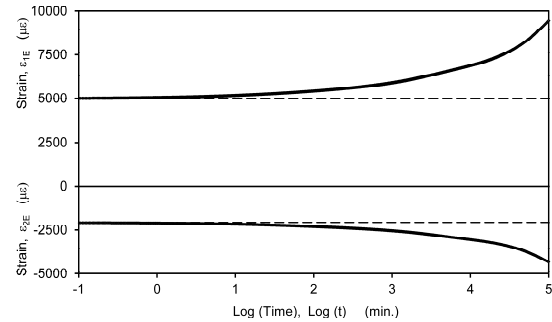


Fig. 2. Directional strains on logarithmic time scale in unidirectional tension creep experimental test on epoxy specimen

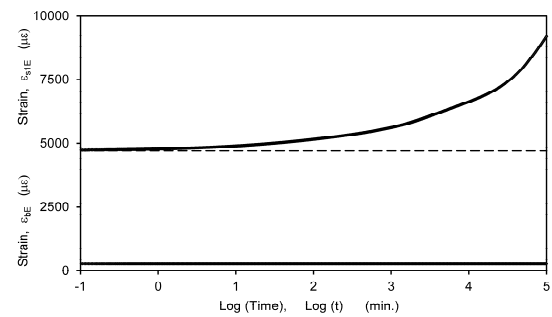


Fig. 3. Shear and bulk strains on logarithmic time scale in unidirectional tension creep experimental test on epoxy specimen

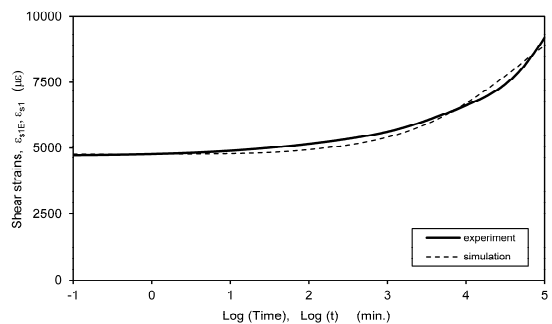


Fig. 4. Simulated shear strain graph  $\epsilon_{s1}(t)$  against experimental shear strain graph  $\epsilon_{s1E}(t)$  in unidirectional tension creep test on epoxy specimen

The results of identifying the viscoelastic constants of the EGS/MHD (glass/epoxy) UFRT composite, using Eqns. (114), (89)<sub>7-10</sub> and reported to 3 significant digits, are as follows:

$$\begin{aligned} c_1 &= 0.0425, & d_1 &= 0.0408, & T_{d_1} &= 65500 \text{ min} \\ c_{23} &= 1.18, & d_{23} &= 0.542, & T_{d_{23}} &= 16700 \text{ min} \\ c_{12} &= 1.22, & d_{12} &= 0.549, & T_{d_{12}} &= 16200 \text{ min} \end{aligned}$$

The H-R/H and VECP storage compliances were calculated according to Eqns. (110)-(112) for  $\alpha \in [2\pi \cdot 0.001, 2\pi \cdot 0.500]$  with step  $\Delta x = 0.001$ . Figure 5 presents the H-R/H storage compliances against the relevant VECP storage compliances. The relative errors are

$$\delta_1 = 0.21 \%, \quad \delta_{23} = 0.05 \%, \quad \delta_{12} = 0.004 \%$$

calculated according to Eqn. (115) for  $P = 500$ . The results prove that the numerical validation of the H-R/H rheological model is positive for UFRT composites reinforced with isotropic (glass) fibres.

The results of identifying the viscoelastic constants of the T300/BSL (carbon/epoxy) UFRT composite, using Eqns. (114), (89)<sub>7-10</sub> and reported to 3 significant digits, are as follows:

$$\begin{aligned} c_1 &= 0.0145, & d_1 &= 0.0143, & T_{d_1} &= 68900 \text{ min} \\ c_{23} &= 0.716, & d_{23} &= 0.417, & T_{d_{23}} &= 26000 \text{ min} \\ c_{12} &= 1.03, & d_{12} &= 0.508, & T_{d_{12}} &= 19000 \text{ min} \end{aligned}$$

The H-R/H and VECP storage compliances were calculated according to Eqns. (110)-(112) for  $\alpha \in [2\pi \cdot 0.001, 2\pi \cdot 0.500]$  with step  $\Delta x = 0.001$ . Figure 6 presents the H-R/H storage compliances against the relevant VECP storage compliances. The relative errors are

$$\delta_1 = 0.08\%, \quad \delta_{23} = 0.14\%, \quad \delta_{12} = 0.02\%$$

calculated according to Eqn. (115) for  $P = 500$ .

The results prove that the numerical validation of the H-R/H rheological model is positive for UFRT composites reinforced with monotropic (carbon) fibres.

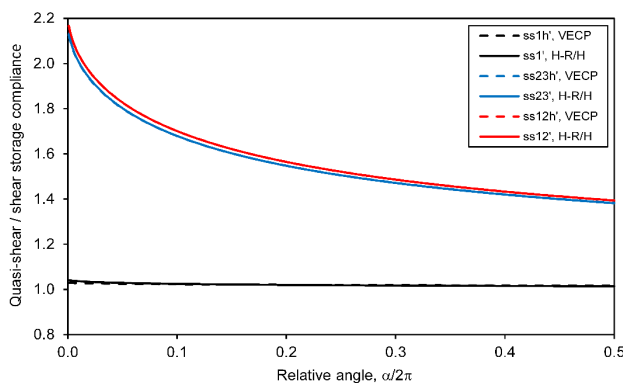


Fig. 5. H-R/H storage compliances  $s'_{s1}(\alpha), s'_{s23}(\alpha), s'_{s12}(\alpha)$  against VECP storage compliances  $s_{s1h}(\alpha), s_{s23h}(\alpha), s_{s12h}(\alpha)$  for EGS/MHD composite

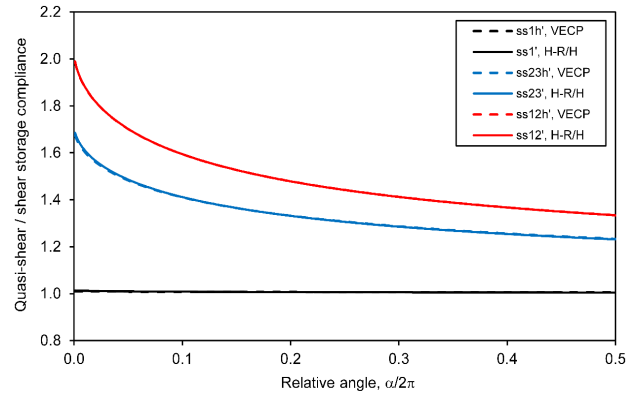


Fig. 6. H-R/H storage compliance  $s'_{s1}(\alpha), s'_{s23}(\alpha), s'_{s12}(\alpha)$  against VECP storage compliance  $s_{s1h}(\alpha), s_{s23h}(\alpha), s_{s12h}(\alpha)$  for T300/BSL composite

Given the negligibly small values of viscoelastic constant  $c_1$  compared to unity as evidenced in this Section,  $c_1 = 0$  can be assumed. The number of independent effective viscoelastic constants describing a UFRT composite reduces then to four, i.e.  $T_c, r, c_{23}, c_{12}$ . In Eqns. (82)<sub>1</sub>, (88)<sub>1</sub>, (96), one should assume

$$\begin{aligned} S_{s1}(t) &= S_{s1e}, & C_{s1}(t) &= C_{s1e}, \\ S_{v1}(t) &= 0, & C_{v1}(t) &= 0 \end{aligned} \quad (116)$$

Based on the simulated exemplary UFRT materials, the following final conclusions can be formulated:

- The H-R/H rheological model is adequate for thermosets in the technically relevant interval  $t \in [0, 10^5 \text{ min}]$ .
- The H-R/H rheological model is adequate for UFRT composites in the technically relevant interval  $t \in [0, 10^5 \text{ min}]$ .
- Two viscoelastic constants, i.e. retardation time  $T_c$  and fraction  $r$ , are common to the thermoset matrix and the UFRT composite.
- Shear creep in the monotropy and transverse isotropy planes of UFRT composites is dominant. The elastic fibres are very effective at suppressing the viscoelastic effects in UFRT composites under tension/compression in the fibre direction.

## CONCLUSIONS

Refined fully analytical modelling of the linear rheology of thermosets and unidirectional monotropic fibre-reinforced thermoset matrix (UFRT) composites was developed. The components of a UFRT composite were assumed to be a linearly elastic-viscoelastic isotropic material (matrix) and a linearly elastic monotropic material (fibre). The homogenized UFRT composite was assumed to be a linearly elastic-viscoelastic monotropic material. All the solutions as well as the all the transformations transforming one quantity/equation into another are analytical.

New rheological models labelled H-R/H for thermosets and UFRT composites with monotropic fibres are described by the smallest possible numbers of the material constants. A single Mittag-Leffler fractional exponential generic function in an integral form, common to the thermoset matrix and the homogenized UFRT composite, guarantees prediction of the rheological processes with good accuracy. The H-R/H model of a thermoset was described by two independent elastic constants  $(E_m, \nu_m)$  and three independent viscoelastic constants  $(T_c, r, c)$ . The H-R/H model of the homogenized UFRT composite was described by five independent elastic constants  $(E_1, E_2, \nu_{12}, \nu_{23}, G_{12})$  and four independent viscoelastic constants  $(T_c, r, c_{23}, c_{12})$ , whereby constants  $T_c, r$  are common to the thermoset matrix and the UFRT composite.

The refined analytical constitutive modelling of the linear rheology of thermosets was validated positively on the selected epoxy resin. The considerations were limited to quasi-static isothermal reversible rheological processes. Further development would require comprehensive elastic and rheological experiments on selected thermosetting polymers, taking into account the effects of the stress level, temperature, time and material ageing.

The improved homogenization theory and the refined analytical constitutive modelling of the linear rheology of UFRT composites were validated positively on selected increased reliability UFRT composites taken from [31, 32]. The considerations were limited to quasi-static isothermal reversible rheological processes.

The most important, new and original elements in the presented study are as follows:

- formulation of the refined rheological modelling of thermosets,
- formulation of the improved homogenization theory of UFRT composites with monotropic fibres,
- formulation of the refined rheological modelling of UFRT composites with monotropic fibres,
- formulation of the H-R/H rheological models that describe thermosets and UFRT composites by the smallest possible numbers of elastic and viscoelastic constants,
- experimental validation of the improved homogenization theory on selected increased reliability UFRT composites,
- experimental validation of the H-R/H rheological model of thermosets carried out on selected epoxy resin,
- numerical validation of the H-R/H rheological model of UFRT composites carried out on selected increased reliability UFRT composites with monotropic or isotropic fibres.

Further development of the elasticity and rheology of UFRT composites would require comprehensive elastic and rheological experiments on selected composites, taking into account the effects of the stress level, temperature, time and material ageing.

## APPENDIX A. SELECTED MATHEMATICAL FORMULAS [2, 29]

Functions  $L(u), \Phi(t), \varphi(t)$  have the following properties:

$$\begin{aligned} L(u) \geq 0 \text{ for } u \geq 0, \quad \int_0^\infty L(u) du = 1, \quad \lim_{u \rightarrow 0^+} L(u) = \infty \\ \Phi(t) > 0 \text{ for } t > 0, \quad \lim_{t \rightarrow 0^+} \Phi(t) = \infty, \quad \lim_{t \rightarrow \infty} \Phi(t) = 0 \\ \varphi(0) = 0, \quad \varphi(\infty) = \lim_{t \rightarrow \infty} \varphi(t) = 1 \end{aligned} \quad (\text{A.1})$$

The initial creep velocity of a thermoset corresponding to the H-R/H rheological model has an infinite value, i.e.

$$\dot{\varphi}(t) = \frac{d\varphi(t)}{dt} = \Phi(t), \quad \dot{\varphi}(0) = \lim_{t \rightarrow 0^+} \Phi(t) = \infty \quad (\text{A.2})$$

For  $t > 0$ , velocity  $\dot{\varphi}(t)$  drops sharply to a low value, as observed in the experimental tests.

The shear storage and loss compliances that describe the rheological properties of a thermoset have the following properties:

$$\begin{aligned} S'_s(\omega) > 0, \quad S'_s(0) = (1+c)S_s, \quad \lim_{\omega \rightarrow \infty} S'_s(\omega) = S_s \\ S''_s(\omega) < 0 \text{ for } \omega > 0, \quad S''_s(0) = 0, \quad \lim_{\omega \rightarrow \infty} S''_s(\omega) = 0 \end{aligned} \quad (\text{A.3})$$

When  $r \rightarrow 1$ , a Mittag-Leffler generic function becomes a normal exponential function, i.e.

$$\begin{aligned} L(u) = \delta(u-1), \quad \Phi(t) = \frac{1}{T_c} \exp\left(-\frac{t}{T_c}\right), \\ \Psi(t) = \frac{1}{T_d} \exp\left(-\frac{t}{T_d}\right) \end{aligned} \quad (\text{A.4})$$

where  $\delta(u-1)$  is a Dirac function. The final equations for case  $r \rightarrow 1$ , useful for comparative purposes, are collected below:

- creep/relaxation functions:

$$\varphi(t) = 1 - \exp(-t/T_c), \quad \psi(t) = 1 - \exp(-t/T_d) \quad (\text{A.5})$$

- time conversion:

$$T_d = T_c / (1+c) \quad (\text{A.6})$$

- Laplace transforms of generic functions:

$$\bar{\Phi}(q) = \frac{1}{1+qT_c}, \quad \bar{\Psi}(q) = \frac{1}{1+qT_d} \quad (\text{A.7})$$

- shear storage and loss compliances:

$$\begin{aligned} S'_s(\omega) = S_{se} \left[ 1 + c \frac{1}{1+(\omega T_c)^2} \right], \\ S''_s(\omega) = -S_{se} c \frac{\omega T_c}{1+(\omega T_c)^2} \end{aligned} \quad (\text{A.8})$$

Equations (A.4)-(A.8) describe the H-K/H rheological model (standard model) of an isotropic material.

## Acknowledgements

*The experimental unidirectional tension creep test on epoxy resin was conducted in 2002 at the Materials*

and Structures Research Laboratory, Faculty of Mechanical Engineering, Military University of Technology, Warsaw, Poland, as a part of research project No. 7 T08E 011 18, which received funding from the Scientific Research Committee, Poland. This support is gratefully acknowledged.

## REFERENCES

- [1] Klasztorny M., Nycz D.B., Bogusz P., Rheological effects in in-plane shear test and in-plane shear creep test on glass-vinyl-ester lamina, *Composites Theory and Practice* 2020, 20, 1, 35-42. [https://kompozyty.ptmk.net/pliczki/pliki/1338\\_2020t01\\_marian-klasztorny-daniel-b-.pdf](https://kompozyty.ptmk.net/pliczki/pliki/1338_2020t01_marian-klasztorny-daniel-b-.pdf).
- [2] Klasztorny M., Nycz D.B., Modelling of linear elasticity and viscoelasticity of thermosets and unidirectional-fibre-reinforced thermoset-matrix composites – Part 1: Theory of modelling, *Composites Theory and Practice* 2022, 22, 1, 3-15. [https://kompozyty.ptmk.net/pliczki/pliki/1382\\_2022t01\\_marian-klasztorny-daniel-b-.pdf](https://kompozyty.ptmk.net/pliczki/pliki/1382_2022t01_marian-klasztorny-daniel-b-.pdf).
- [3] Rabotnov J.N., *Creep of elements of structures* [in Russian], Nauka Press, Moscow 1966.
- [4] Schapery R.A., On the characterization of nonlinear viscoelastic materials, *Polymer Engineering Science* 1969, 9, 295-310.
- [5] Aboudi J., Micromechanical characterization of the nonlinear viscoelastic behaviour of resin matrix composites, *Composites Science and Technology* 1990, 38, 4, 371-386.
- [6] Papanicolaou G.C., Zautsos S.P., Cardon A.H., Further development of a data reduction method for the nonlinear viscoelastic characterization of FRPs, *Composites Part A* 1999, 30, 7, 839-848, DOI: 10.1016/S1359-835X(99)00004-4.
- [7] Haj-Ali R., Muliana A., A micro-to-meso sublaminar model for the viscoelastic analysis of thick-section multi-layered FRP composite structures, *Mechanics of Time-Dependent Materials* 2008, 12, 1, 69-93, DOI: 10.1007/s11043-007-9041-6.
- [8] Falahatgar S.R., Salehi M., Nonlinear viscoelastic response of unidirectional polymeric laminated composite plates under bending loads, *Applied Composite Materials* 2011, 18, 6, 471-483, DOI: 10.1007/s10443-011-9212-0.
- [9] Jeon J., Kim J., Muliana A., Modeling time-dependent and inelastic response of fiber reinforced polymer composites, *Computational Materials Science* 2013, 70, 37-50, DOI: 10.1016/j.commatsci.2012.12.022.
- [10] Nunes S.G., Saseendran S., Joffe R. et al., On temperature-related shift factors and master curves in viscoelastic constitutive models for thermoset polymers, *Mechanics of Composite Materials* 2020, 56, 5, 573-590, DOI: 10.1007/s11029-020-09905-2.
- [11] Kontou E., Tensile creep behavior of unidirectional glass-fiber polymer composites, *Polymer Composites* 2005, 26, 3, 287-292, DOI: 10.1002/pc.20098.
- [12] Starkova O., Anishevich A., Limits of linear viscoelastic behavior of polymers, *Mechanics of Time-Dependent Materials* 2007, 11, 2, 111-126, DOI: 10.1007/s11043-007-9036-3.
- [13] Muliana A.H., Sawant S., Responses of viscoelastic polymer composites with temperature and time dependent constituents, *Acta Mechanica* 2009, 204, 3, 155-173. DOI: 10.1007/s00707-008-0052-4.
- [14] Ascione L., Berardi V.P., D'Aponte A., A viscoelastic constitutive law for FRP materials, *International Journal of Computational Methods in Engineering Science and Mechanics* 2011, 12, 5, 225-232, DOI: 10.1080/15502281003660211.
- [15] Zhang X., Huang Q., Chen J. et al., Prediction of viscoelastic behavior of unidirectional polymer matrix composites, *Journal of Wuhan University of Technology: Materials Science Edition* 2016, 31, 3, 695-699, DOI: 10.1007/s11595-016-1431-7.
- [16] Kotelnikova-Weiler N., Baverel O., Ducoulombier N. et al., Progressive damage of a unidirectional composite with a viscoelastic matrix, observations and modelling, *Composite Structures* 2018, 188, 297-312, DOI: 10.1016/j.compstruct.2017.12.067.
- [17] Cardoso D.C.T., Harries K.A., A viscoelastic model for time-dependent behavior of pultruded GFRP, *Construction and Building Materials* 2019, 208, 63-74, DOI: 10.1016/j.conbuildmat.2019.02.155.
- [18] Berardi V.P., Perrella M., Armentani E. et al., Experimental investigation and numerical modeling of creep response of glass fiber reinforced polymer composites, *Fatigue Fract. Eng. M* 2021, 44, 4, 1085-1095, DOI: 10.1111/ffe.13415.
- [19] Di Gennaro L., Daghia F., Olive M. et al., A new mechanism-based temperature-dependent viscoelastic model for unidirectional polymer matrix composites based on Cartan decomposition, *European Journal of Mechanics A – Solids* 2021, 90, 104364, DOI: 10.1016/j.euromechsol.2021.104364.
- [20] Wilczynski A.P., Klasztorny M., Determination of complex compliances of fibrous polymeric composites, *Journal of Composite Materials* 2000, 34, 1, 2-26, DOI: 10.1177/002199830003400101.
- [21] Klasztorny M., Wilczynski A.P., Constitutive equations of viscoelasticity and estimation of viscoelastic parameters of unidirectional fibrous polymeric composites, *Journal of Composite Materials* 2000, 34, 19, 1624-1639, DOI: 10.1106/K8KV-7NEN-5Q04-G217.
- [22] Klasztorny M., Wilczynski A.P., Wittemberg-Perzyk D., A rheological model of polymeric materials and identification of its parameters, *J Theor App Mech-Pol* 2001, 39, 1, 13-32. <http://www.ptmts.org.pl/jtam/index.php/jtam/issue/view/v39n1>.
- [23] Wilczynski A.P., Klasztorny M., Modelling of fibrous polymeric composites in the viscoelastic range [in Polish], *Kompozyty (Composites)* 2002, 2, 3, 97-102. [https://kompozyty.ptmk.net/pliczki/pliki/semVI\\_16.pdf](https://kompozyty.ptmk.net/pliczki/pliki/semVI_16.pdf).
- [24] Klasztorny M., Gieleta R., Modelling of viscoelastic resins as matrices of fibre-reinforced polymeric composites [in Polish], *Kompozyty (Composites)* 2002, 2, 3, 103-107, [https://kompozyty.ptmk.net/pliczki/pliki/semVI\\_17.pdf](https://kompozyty.ptmk.net/pliczki/pliki/semVI_17.pdf).
- [25] Klasztorny M., Gieleta R., The HWKK rheological model for resins, *J. Theor. App. Mech.-Pol.* 2002, 40, 4, 939-960, <http://www.ptmts.org.pl/jtam/index.php/jtam/issue/view/v40n4>.
- [26] Klasztorny M., Constitutive modelling of resins in compliance domain, *Mechanics of Composite Materials* 2004, 40, 4, 349-358, DOI: 10.1023/B:MOCM.0000039751.74145.63.
- [27] Klasztorny M., Constitutive modelling of resins in stiffness domain, *Mechanics of Composite Materials* 2004, 40, 5, 443-452, DOI: 10.1023/B:MOCM.0000047235.48540.fc.
- [28] Klasztorny M., Numerical simulation of rheological processes in hardening plastics under stress control, *Mechanics of Composite Materials* 2007, 43, 2, 133-140, DOI: 10.1007/s11029-007-0014-2.
- [29] Klasztorny M., Nycz D.B., Modelling of linear elasticity and viscoelasticity of thermosets and unidirectional-fibre-reinforced thermoset-matrix composites – Part 2: Homogenization and numerical analysis, *Composites Theory and Practice* 2022, 22, 1, 25-39, [https://kompozyty.ptmk.net/pliczki/pliki/1385\\_2022t01\\_marian-klasztorny-daniel-b-.pdf](https://kompozyty.ptmk.net/pliczki/pliki/1385_2022t01_marian-klasztorny-daniel-b-.pdf).

- [30] Kłasztorny M., Konderla P., Piekarski R., An exact stiffness theory for unidirectional xFRP composites, *Mechanics of Composite Materials* 2009, 45, 1, 77-104, DOI: 10.1007/s11029-009-9064-y.
- [31] Soden P.D., Hinton M.J., Kaddour A.S., Lamina properties, lay-up configurations and loading conditions for a range of fibre-reinforced composite laminates, *Composites Science and Technology* 1998, 58, 7, 1011-1022, DOI: 10.1016/S0266-3538(98)00078-5.
- [32] Soden P.D., Hinton M.J., Kaddour A.S., Biaxial test results for strength and deformation of a range of E-glass and carbon fibre reinforced composite laminates: failure exercise benchmark data, *Composites Science and Technology* 2002, 62, 1489-1514, DOI: 10.1016/S0266-3538(02)00093-3.
- [33] Wilczynski A.P., A basic theory of reinforcement for unidirectional fibrous composites, *Composites Science and Technology* 1990, 38, 4, 327-337, DOI: 10.1016/0266-3538(90)90019-2.
- [34] Wilczynski A.P., Lewinski J., Predicting the properties of unidirectional fibrous composites with monotropic reinforcement, *Composites Science and Technology* 1995, 55, 2, 139-143, DOI: 10.1016/0266-3538(95)00090-9.
- [35] Kłasztorny M., Urbanski A., Application of the finite element method to improve quasi-exact reinforcement theory of fibrous polymeric composites, *Mechanics of Composite Materials* 2005, 41, 1, 55-64, DOI: 10.1007/s11029-005-0007-y.
- [36] Daniel I.M., Ishai O., *Engineering Mechanics of Composite Materials*, Oxford University Press, New York-Oxford 1994.
- [37] Kłasztorny M., Coupled and uncoupled constitutive equations of linear elasticity and viscoelasticity of orthotropic materials, *J. Theor. App. Mech.-Pol.* 2008, 46, 1, 3-20, <https://www-1webofscience-1com-100003ee80000.han.wat.edu.pl/wos/woscc/full-record/WOS:000258574900001>.
- [38] EfunDA Engineering Fundamentals. Abscissas and Weights of Gauss-Legendre Integration, [https://www.efunda.com/math/num\\_integration/findgausslegendre.cfm](https://www.efunda.com/math/num_integration/findgausslegendre.cfm) (accessed 15.05.2021).